

A HYBRID PHYSICS-INFORMED NEURAL NETWORK BASED MULTISCALE SOLVER AS A PARTIAL DIFFERENTIAL EQUATION CONSTRAINED OPTIMIZATION PROBLEM*

MICHAEL HINTERMÜLLER^{‡†} AND DENIS KOROLEV[‡]

Abstract. In this work, we study physics-informed neural networks (PINNs) constrained by partial differential equations (PDEs) and their application in approximating PDEs with two characteristic scales. From a continuous perspective, our formulation corresponds to a non-standard PDE-constrained optimization problem with a PINN-type objective. From a discrete standpoint, the formulation represents a hybrid numerical solver that utilizes both neural networks and finite elements. For the problem analysis, we introduce a proper function space, and we develop a numerical solution algorithm. The latter combines an adjoint-based technique for the efficient gradient computation with automatic differentiation. This new multiscale method is then applied exemplarily to a heat transfer problem with oscillating coefficients. In this context, the neural network approximates a fine-scale problem, and a coarse-scale problem constrains the associated learning process. We demonstrate that incorporating coarse-scale information into the neural network training process via a weak convergence-based regularization term is beneficial. Indeed, while preserving upscaling consistency, this term encourages non-trivial PINN solutions and also acts as a preconditioner for the low-frequency component of the fine-scale PDE, resulting in improved convergence properties of the PINN method.

Key words. Learning-informed optimal control, PDE constrained optimization, physics-informed neural networks, quasi-minimization, weak convergence, multiscale modelling

MSC codes. 35B27, 65K10, 65J15, 65N99, 68T20, 80M40

1. Introduction. Solving partial differential equations (PDEs) using physics-informed neural networks (PINNs) is currently an active area of research; see, e.g. [15] for an overview and references therein. The main principle of physics-informed learning was pioneered by [43] and later reincarnated in its modern computational interpretation by Raissi *et al.* [56]. It consists of integrating physical laws, typically in the form of the residuals of underlying PDEs, into a least-squares objective and finding the approximate solution to the corresponding residual minimization problem. The approximation ansatz $u_{\theta,n}$ for the PDE solution $u \in U$, with U a suitable Banach space, is then sought in a neural network class $\mathfrak{N}_{\theta,n}$. The unknown network parameters $\theta \in \mathbb{R}^{N_n}$, the so-called weights and biases, are determined by solving an associated nonlinear and non-convex optimization problem. PINN methods are typically meshless, rendering them potentially useful for numerically solving PDEs on complex domains or in high dimensions [32, 72]. The associated framework is rather flexible and allows for easy data incorporation in various ways, making PINNs not only versatile, but also a competitive approach for solving inverse problems [13, 36, 50]. In addition, the expressiveness of neural networks is supported by universal approximation theorems [17, 29, 49, 69, 71] and transfer learning capabilities [26, 70]. Moreover, (approximate) optimization can be performed rapidly on modern computers and compute clusters, thanks to the excellent parallelization capabilities of neural networks on

*Submitted to the editors DATE.

Funding: The authors acknowledge the support of the Leibniz Collaborative Excellence Cluster under project ML4Sim (funding reference: K377/2021). MH also acknowledges support by the DFG ExC 2046 MATH+: Berlin Mathematics Research Center under project EF1-17.

[†]Institute for Mathematics, Humboldt-Universität zu Berlin, Unter den Linden 6, 10099 Berlin, Germany (hint@mathematik.hu-berlin.de)

[‡]Weierstrass Institute for Applied Analysis and Stochastics (WIAS), Mohrenstr. 39, 10117 Berlin, Germany (korolev@wias-berlin.de, hintermueller@wias-berlin.de).

GPUs, advances in automatic differentiation, as well as parallel and domain decomposition techniques [35, 52, 58]. On the other hand, the non-convex nature of the underlying optimization and complex nonlinear dynamics within the learning process often lead to difficulties and limitations rendering the analytical and numerical handling delicate [64, 66]. Furthermore, PINNs can be difficult to train for problems exhibiting high-frequency or multiscale behavior [65], particularly due to the so-called “spectral bias” of neural networks. The latter is related to the fact that learning prioritizes low-frequency modes and prevents networks from effectively learning high-frequency functions [55]. However, the combination of physics-informed neural networks with numerically robust and efficient solvers may yield a way to mitigate these challenges.

Motivated by multiscale systems, in this work we enhance neural network training by incorporating a learning-informed PDE as a constraint into the PINN optimization. For the ease of exposition, we consider here a two-scale setting only, which involves a fine-scale equation (of formidable computational complexity, perhaps beyond reach) and a coarse-scale equation (which we consider computationally tractable). The aforementioned computational burden may stem, e.g., from fine-scale properties of composite materials (foams, textiles, etc) resulting in highly oscillatory multiscale or high-contrast coefficients (heat conductivity, permeability, etc). A reliable associated simulation may then require a prohibitively fine numerical resolution. In order to remedy the enormous computational complexity, we use a neural network based approximation of the fine-scale problem which informs the coarse-scale problem through a homogenization procedure of choice. This gives rise to the following PDE-constrained optimization problem:

$$(1.1) \quad \begin{cases} \inf J(y, u_{\theta,n}) & \text{over } (y, u_{\theta,n}), \\ \text{subject to (s.t.) } \mathcal{L}[u_{\theta,n}]y = f, \end{cases}$$

where J stands for a (least-squares) loss functional penalizing the PDE residual of the fine-scale equation (possibly including boundary conditions). It is worth noting that in the standard PINN framework, J depends solely on $u_{\theta,n}$. Here, however, we also introduce a coupling term to make the loss also dependent on y , thus stabilizing the training by the aforementioned coarse-scale enrichment. Conceptually, this additional term incorporates information on the weak convergence of the fine-scale solution to the coarse-scale one into the loss functional. By $\mathcal{L}[u_{\theta,n}] : Y \rightarrow Z$ we denote a coarse-scale differential operator between Banach spaces Y and Z , which is informed by our neural network ansatz yielding $u_{\theta,n}$. Together with some given data f , it defines an equality constraint in (1.1). Structurally, $u_{\theta,n}$ may be considered a control variable, whereas the coarse-scale solution y acts as a state. The abstract framework is quite general, allowing for the use of various (multiscale) techniques to parameterize $\mathcal{L}[u_{\theta,n}]$ by $u_{\theta,n}$.

In the realm of learning-informed optimal control, several works, including [19, 59], have focused on approximating nonlinear constituents or source terms in the state equation using neural networks. PINNs have also been employed in solvers for underlying state and adjoint equations in various PDE-constrained optimization scenarios [47, 53]. In [10], the neural stabilization of non-stable discrete weak formulations is proposed, resulting in a non-standard PDE-constrained optimization with neural network controls. Let us point out here that all the aforementioned techniques, while structurally perhaps similar, differ from this work. Indeed, in the usual approaches the objective is typically not related to a neural network learning problem or PDE residual minimization, but rather to minimizing specific (e.g., tracking-type) cost

functionals [11, 31]. This difference has significant implications in analysis and numerical implementation. Besides, to the best of the authors' knowledge, our work is the first to deal in detail with a PINN-based optimization problem constrained by a PDE. Here, problem (1.1) is formulated and analyzed in a function space setting, taking into account the regularity of the fine-scale and coarse-scale PDE solutions as well as the interdependent choices of activation functions and PINN losses. For our new problem (1.1), the concept of quasi-minimization [57] is crucial when studying (approximate) existence of solutions.

Discretizing the coarse-scale equation in (1.1), e.g., via the finite element method, alongside a (meshless) PINN-based approach for the fine-scale problem, yields a *hybrid physics-informed multiscale* numerical solver. In this context, the meshless approach appears particularly useful for complex geometries. Note also that in the course of the optimization process for solving the hybrid finite dimensional approximate version of (1.1) possibly requires to frequently solve the discretized coarse-scale PDE. The hope now is that the coarse-scale equation can be solved numerically at a significantly lower cost (compute time) than computing the PINN solution, while still well informing low-frequency components of the fine-scale solution. Our numerical experiments provide evidence that incorporating the coarse-scale solution into the learning process through a coupling term in the objective of (1.1) acts as a preconditioner for the low-frequency component of the fine-scale PDE, thereby accelerating convergence to such a component and improving the overall performance. The proposed methodology can be used with most PINN architectures (standard PINNs [56], Fourier features networks [61, 65], FBPINNs [52], etc) and has the potential to improve existing benchmarks.

PINNs find numerous applications in multiscale systems and material design (see, e.g., [13, 18, 47, 74]). Some NN-based homogenization techniques [4, 30, 41], including PINN-based approaches [44, 54], have also been proposed. Besides, it is worth noting that decades of research in multiscale modelling have yielded powerful methods for obtaining surrogates at the coarse scale (see, e.g., [1, 21, 34, 48, 67]). In our application section, we utilize the upscaling method [23, 68] for numerical homogenization, facilitating the transition from fine-scale to coarse-scale domains via our parametrization $\mathcal{L}[u_{\theta,n}]$. However, despite sharing a similar application context with the aforementioned works, our focus here lies in enhancing PINN approximation for fine-scale problems by integrating it with numerical coarse-scale solvers using multiscale modelling techniques. The resulting hybrid coarse-coarse scale approximation is a byproduct of the neural network approximation on a fine scale and the chosen multiscale coupling, leading to the related *upscaling consistency* concept.

The paper is organized as follows. In Section 2, we introduce an abstract framework for our learning-informed optimization problem. We recall specific details on physics-informed neural networks and introduce a compression operator, which embeds information on weak convergence into our loss function. Then, we derive the related upscaling consistency result. In Section 3, we fit (1.1) into a function space framework and propose a numerical algorithm for its solution. Section 4 presents an upscaling technique for numerical homogenization. We then integrate the upscaling lift into the learning-informed PDE-constrained optimization setting and apply it to the heat transfer problem with oscillating coefficients.

2. A hybrid multiscale approach. In this section, we define a function space and a coupling framework for two PDEs, the fine-scale and the coarse-scale problem, respectively. For the treatment of the associated PINNs, we closely follow [57]. For the bounded domain $\Omega \subset \mathbb{R}^d$ with Lipschitz boundary $\partial\Omega$, let $L^p(\Omega)$, $H^1(\Omega)$, $H_0^1(\Omega)$,

$H^k(\Omega)$, $W^{k,p}(\Omega)$, etc. denote the standard Lebesgue and Sobolev spaces; see, e.g., [2]. We also set $\mathbb{R}_+ := \{x \in \mathbb{R} : x > 0\}$ and $\mathbb{R}_{\geq 0} := \{x \in \mathbb{R} : x \geq 0\}$.

2.1. Function spaces and PDEs. Let $(U, \|\cdot\|_U)$, $(H, \|\cdot\|_H)$ be Hilbert spaces, $(X, \|\cdot\|_X)$ be a normed vector space, $(V, \|\cdot\|_V)$, $(Z, \|\cdot\|_Z)$ be Banach spaces, and X a dense subspace of U . Suppose also that U is continuously embedded in V and V is continuously embedded in H , i.e., $U \hookrightarrow V \hookrightarrow H$. Moreover, $X \hookrightarrow U$.

For given $f^\varepsilon \in H$, we consider the following partial differential equation

$$(2.1) \quad \mathcal{A}^\varepsilon u = f^\varepsilon, \quad \text{in } H, \quad \mathcal{B}u = 0, \quad \text{in } Z,$$

with $\mathcal{A}^\varepsilon : U \rightarrow H$ a bounded linear partial differential operator, i.e., $\mathcal{A}^\varepsilon \in L(U, H)$, depending on the fine-scale length $\varepsilon > 0$, and $\mathcal{B} \in L(U, Z)$ defining boundary conditions. For (2.1) we invoke the following solution concept.

ASSUMPTION 2.1. *For every $\varepsilon > 0$, (2.1) admits a unique solution $u^\varepsilon \in U$ for which there exists an approximating sequence $\{u_k^\varepsilon\} \subset X$ such that*

$$(2.2) \quad \lim_{k \rightarrow \infty} \|u_k^\varepsilon - u^\varepsilon\|_U = 0, \quad \lim_{k \rightarrow \infty} \|\mathcal{A}^\varepsilon u_k^\varepsilon - f^\varepsilon\|_H + \|\mathcal{B}u_k^\varepsilon\|_Z = 0.$$

REMARK 2.2. *Let $g \in Z$ and assume that there exists $u^g \in U$ such that $\mathcal{B}u^g = g$ in Z . If $u^\varepsilon \in U$ satisfies (2.2) with $f^\varepsilon = q - \mathcal{A}^\varepsilon u^g$ for some given $q \in H$, then $w^\varepsilon := u^\varepsilon + u^g \in U$ corresponds to (2.1) with $\mathcal{A}^\varepsilon u = q$ in H and $\mathcal{B}u = g$ in Z .*

From now on we assume that Assumption 2.1 is satisfied. Note that if $u^\varepsilon \in U$ is the solution to (2.1), then $u^\varepsilon \in U_0 := \{u \in U : \mathcal{B}u = 0\} \subseteq U$, and we sometimes use $\|\cdot\|_{U_0}$ instead of $\|\cdot\|_U$. The following stability estimate is standard for least-squares residual minimization, including the least-squares finite element method [6, 7] and physics-informed neural networks [51, 57, 73].

ASSUMPTION 2.3 (Fine-scale stability). *There exist a stability bound $C_s^\varepsilon \in \mathbb{R}_+$ and an upper bound $C_b^\varepsilon \in \mathbb{R}_+$, both possibly dependent on $\varepsilon > 0$, such that*

$$(2.3) \quad C_s^\varepsilon \|u\|_V^2 \leq \|\mathcal{A}^\varepsilon u\|_H^2 + \|\mathcal{B}u\|_Z^2 \leq C_b^\varepsilon \|u\|_U^2, \quad \forall u \in U.$$

The stability bound (2.3) is well-suited for PINN problems which include boundary conditions via penalization. In this case a term penalizing violations of the boundary conditions is added to the PINN objective. Note, however, that boundary conditions may also be imposed exactly, i.e., as (hard) constraints, for PINNS [42, 47, 60]. Then, one may ask (2.3) to hold for all $u \in U_0$, while dropping the term $\|\mathcal{B}u\|_Z^2$ and using a stronger norm $\|\cdot\|_U$ in the lower bound. We demonstrate both approaches in our example section and use (2.3) for our abstract formulation.

Let $(Y, \|\cdot\|_Y)$ be a Hilbert space with $U_0 \subseteq Y$, Y^* the topological dual space of Y and $Y \hookrightarrow H \cong H^* \hookrightarrow Y^*$ a Gelfand triple with the compact embedding $Y \hookrightarrow H$. Let $\mathcal{L}[u] \in L(Y, Y^*)$ be parameterized by $u \in U$. The corresponding bilinear form $b_{\mathcal{L}}[u] : Y \times Y \rightarrow \mathbb{R}$ is defined by

$$(2.4) \quad b_{\mathcal{L}}[u](v, w) := \langle \mathcal{L}[u]v, w \rangle_{Y^*, Y}$$

for $v, w \in Y$. The following assumption is needed to secure (local) solvability of the coarse-scale equation.

ASSUMPTION 2.4 (Coarse-scale stability). *Let $u^\varepsilon \in U$ be the solution of (2.1), $\bar{r}^\varepsilon \in \mathbb{R}_+$ and $B_{\bar{r}^\varepsilon}(u^\varepsilon) := \{v \in U : \|u^\varepsilon - v\|_U \leq \bar{r}^\varepsilon\}$. We assume that the form (2.4)*

is uniformly bounded and uniformly coercive for all $u \in B_{\tilde{r}^\varepsilon}(u^\varepsilon)$, i.e., there exist $C_b^\varepsilon, C_c^\varepsilon \in \mathbb{R}_+$, independent of u , but possibly dependent on ε , such that

$$(2.5) \quad b_{\mathcal{L}}[u](v, w) \leq C_b^\varepsilon \|v\|_Y \|w\|_Y, \text{ and } b_{\mathcal{L}}[u](v, v) \geq C_c^\varepsilon \|v\|_Y^2, \quad \forall v, w \in Y.$$

For given $(u^\varepsilon, \tilde{f}) \in U \times H$, we consider the following partial differential equation, which we refer to as the coarse-scale problem: Find $y(u^\varepsilon) \in Y$ such that

$$(2.6) \quad b_{\mathcal{L}}[u^\varepsilon](y(u^\varepsilon), v) = \langle \tilde{f}, v \rangle_{Y^*, Y} \quad \forall v \in Y.$$

The coarse-scale problem (2.6) is well-posed by the Lax–Milgram lemma. Indeed, there exist a unique solution $y(u^\varepsilon) \in Y$ and a bound $C^\varepsilon \in \mathbb{R}_+$ such that $\|y(u^\varepsilon)\|_Y \leq C^\varepsilon \|\tilde{f}\|_{Y^*}$, with C^ε possibly dependent on ε due to (2.5).

2.2. Physics-informed neural networks. For $L \in \mathbb{N}$, an L -layer feed-forward neural network (NN) is a recursively defined function $R_\theta(x) : \mathbb{R}^{n_0} \rightarrow \mathbb{R}^{n_L}$ with

$$R_\theta(x) = z^L(x), \quad z^l(x) = W^l \sigma(z^{l-1}(x)) + b^l, \quad 2 \leq l \leq L, \quad z^1(x) = W^1 x + b^1,$$

where $W^l \in \mathbb{R}^{n_l \times n_{l-1}}$ is the l -th layer weight matrix, $b_l \in \mathbb{R}^{n_l}$ is the l -th layer bias vector and $\sigma : \mathbb{R} \rightarrow \mathbb{R}$ is the activation function, which is applied component-wise in case of input arguments in \mathbb{R}^{n_l} . The network architecture is represented by the vector $\vec{n} = (n_0, \dots, n_L)$, and the set of all possible network parameters is defined by

$$\Theta(\vec{n}) = \left\{ \{(W_j, b_j)\}_{j=1}^L : W_j \in \mathbb{R}^{n_j \times n_{j-1}}, b_j \in \mathbb{R}^{n_j} \right\}.$$

For a sequence $\{\vec{n}_n\}_{n \geq 1}$ of network architectures such that $\vec{n}_n \leq \vec{n}_{n+1}$ for all n , with the vector inequality understood component-wise, we define its corresponding sequence of neural network classes [57], and the related maximal realization map

$$(2.7) \quad \mathfrak{N}_{\theta, n} := \{R_\theta : \theta \in \cup_{\vec{v} \leq \vec{n}_n} \Theta(\vec{v})\}, \text{ and } \mathfrak{F}_n : \mathbb{R}^{N_n} \rightarrow \mathfrak{N}_{\theta, n}, \quad \theta \mapsto \mathfrak{F}_n(\theta) =: v_{\theta, n},$$

where N_n denotes the total number of parameters in $\Theta(\vec{n}_n)$. Note that $\mathfrak{N}_{\theta, n} \subset \mathfrak{N}_{\theta, n+1}$ by construction, and that the regularity of \mathfrak{F}_n depends on the one of the underlying activation functions in $\mathfrak{N}_{\theta, n}$. In what follows, $v_{\theta, n} \in \mathfrak{N}_{\theta, n}$ refers to a network function, generated by its maximal admissible number of parameters N_n .

The residual minimization of the fine-scale PDE over the class of neural networks leads to the following PINN optimization problem:

$$(2.8) \quad \inf \mathcal{J}(v_{\theta, n}) := \|\mathcal{A}^\varepsilon v_{\theta, n} - f^\varepsilon\|_H^2 + \tau_1 \|\mathcal{B} v_{\theta, n}\|_Z^2 \quad \text{over } v_{\theta, n} \in \mathfrak{N}_{\theta, n},$$

where the penalty parameter $\tau_1 > 0$ is fixed. We observe that $\mathcal{J}(u) \geq 0$ for all $u \in U$, and $\mathcal{J}(u^\varepsilon) = 0$ for the solution u^ε to (2.1). Assuming momentarily that $U = H^2(\Omega)$ and \mathcal{A}^ε is of second order, we need to ensure that u^ε can be approximated by a neural network. It is well-known that Sobolev functions can be well approximated via popular deep ReLU neural networks; see, e.g., [29]. Note, however, that the ReLU activation function $\sigma(x) = \max(0, x)$ admits only one weak derivative, which renders it infeasible when utilizing the standard least-squares loss with $H = L^2(\Omega)$ and \mathcal{A}^ε involving higher-order (weak) derivatives. The hyperbolic tangent function $\tanh(x)$ can then be used to approximate functions from Sobolev spaces $H^k(\Omega)$, $k \geq 3$, in the norm of U (see [16, Theorem B.7], but also [17]). We mention that the regularity requirements on activation functions and u^ε can be relaxed by adopting a variational loss function [38, 39]. This involves multiplying the residuals of (2.1) by suitably smooth test

functions and integrating by parts. Then, the respective weak residual is minimized over a (discrete) trial class of neural networks. In such a setting, one is confronted with the additional burden of discretizing the space of test functions. Typically, piecewise polynomials of low order, leading to a Petrov-Galerkin discretization, are preferred [5]. Moreover, the Fourier transform can be employed to efficiently evaluate the H^{-1} norm of the PDE residual for simple geometries [62].

In view of the above, in our work we focus on a setting with smooth activation functions. Instead of imposing assumptions on the sufficiently high number of admissible weak derivatives of u^ε , we rather work in a dense subspace X of U , where the approximation with neural networks is less restrictive, such as $X = C^k(\bar{\Omega})$, which motivates the triplet of spaces $\mathfrak{N}_{\theta,n} \subset X \subset U$ and our definition of solution (2.2). Then, we are interested in neural networks that can well approximate elements in X ; cf. [57] and some universal approximation results [17, 29, 49, 69, 71].

ASSUMPTION 2.5 (Uniform NN approximation of elements in X). *There exists a sequence of neural network classes $\{\mathfrak{N}_{\theta,n}\}$ with $\mathfrak{N}_{\theta,n} \subset X$ and $\mathfrak{N}_{\theta,n} \subset \mathfrak{N}_{\theta,n+1}$ for all $n \in \mathbb{N}$, and $X \subset \cup_n \mathfrak{N}_{\theta,n}$ in the topology of $(X, \|\cdot\|_X)$. In addition, it holds that $\mathcal{A}^\varepsilon v_{\theta,n} \in L^2(\Omega)$ and $Bv_{\theta,n} \in L^2(\partial\Omega)$ for all $v_{\theta,n} \in \mathfrak{N}_{\theta,n}$.*

2.3. Weak convergence based regularization. Let $H = L^2(\Omega)$ and $H^\delta := L^2(\Omega_\delta)$, where $\Omega_\delta := \{z \in \Omega : \text{dist}(z, \partial\Omega) > \frac{\delta}{2}\} \subset \Omega$ for $\delta > 0$. The weak convergence assumption is common in the context of homogenization, and we make use of the following.

ASSUMPTION 2.6 (Weak convergence). *Assume that for $\gamma > 0$, $u^\varepsilon \rightharpoonup y^0$ in $L^{2+\gamma}(\Omega)$ as $\varepsilon \rightarrow 0$, where u^ε is the solution to (2.1) and $y^0 \in Y$ is the solution to the homogenized equation $\mathcal{L}^0 y^0 = f^0$, with $\mathcal{L}^0 \in L(Y, Y^*)$ and $f^0 \in H$ ε -independent, respectively.*

REMARK 2.7. *In our setting, f^ε in (2.1), \tilde{f} in (2.6), and f^0 in Assumption 2.6 are different in general. This is due to the lifting of Dirichlet boundary conditions in all the PDEs, cf. Remark 2.2. Besides, we assume that y^0 has at least the same regularity as $y(u^\varepsilon)$, as it follows from Assumption 2.6 and our choice of spaces.*

In addition, we need the following; cf. e.g. [1, Theorem 4.5] or [68, Section 3.2].

ASSUMPTION 2.8 (Consistent parametrization). *There exist $C_{\mathcal{L}[u]}, C_\varepsilon \in \mathbb{R}_+$ such that $\|y^0 - y(u^\varepsilon)\|_H \leq C_{\mathcal{L}[u]} + C_\varepsilon$, where $C_{\mathcal{L}[u]}$ does not depend on ε and can be made small by an appropriate parametrization of $y(u^\varepsilon)$ by u^ε , and $C_\varepsilon \rightarrow 0$ as $\varepsilon \rightarrow 0$.*

For $v \in H$, $x \in \Omega_\delta$ and $\mathcal{V}_\delta(x) = \{z : \|z - x\|_{\mathbb{R}^d} \leq \frac{\delta}{2}\} \subset \Omega$, define $Q_\delta : H \rightarrow H^\delta$ by

$$(Q_\delta v)(x) := \frac{1}{|\mathcal{V}_\delta(x)|} \int_{\mathcal{V}_\delta(x)} v(z) dz.$$

Following heterogeneous multiscale methods [1], we fix the compression operator

$$(2.9) \quad (\bar{Q}_\delta v)(x) := \begin{cases} (Q_\delta v)(x), & x \in \Omega_\delta, \\ v(x), & x \in \Omega \setminus \Omega_\delta. \end{cases}$$

Let us next introduce the coupling term $\mathcal{R}_\delta : Y \times U \rightarrow \mathbb{R}_{\geq 0}$ as follows:

$$(2.10) \quad \mathcal{R}_\delta(y(u^\varepsilon), u^\varepsilon) := \|\bar{Q}_\delta u^\varepsilon - y(u^\varepsilon)\|_H^2.$$

The purpose of (2.10) is to equip the optimization problem (2.8) with information on weak convergence of the fine-scale solution to the coarse-scale one.

Next we study (2.10). We start with two preparatory result.

LEMMA 2.9. *The operator $Q_\delta : H \rightarrow H^\delta$ has the following properties:*

1. $Q_\delta \in L(H, H^\delta)$ and $\bar{Q}_\delta \in L(H) := L(H, H)$.
2. Suppose that $u^\varepsilon \rightharpoonup y^0$ in H as $\varepsilon \rightarrow 0$. Then, $\lim_{\varepsilon \rightarrow 0} \|Q_\delta u^\varepsilon - Q_\delta y^0\|_{H^\delta} = 0$.

Proof. The linearity of Q_δ is obvious. For $x \in \Omega_\delta$, using the Cauchy–Schwarz inequality, we obtain the estimate $|(Q_\delta u^\varepsilon)(x)| \leq |\mathcal{V}_\delta(x)|^{-1/2} \|u^\varepsilon\|_H$. Since $|\mathcal{V}_\delta(x)|$ is constant for all $x \in \Omega_\delta$, the estimate is uniform. By integrating the estimate over Ω_δ , we get $\|Q_\delta u^\varepsilon\|_{H^\delta} \leq C \|u^\varepsilon\|_H$, where $C \in \mathbb{R}_+$. Therefore, $Q_\delta \in L(H, H^\delta)$ and we readily establish that $\bar{Q}_\delta \in L(H)$.

Let $u^\varepsilon \rightharpoonup y^0$ in H as $\varepsilon \rightarrow 0$. Then $\|u^\varepsilon\|_H \leq C$, where $C \in \mathbb{R}_+$ is ε -independent, and for all test functions $v \in H$ it holds that

$$(2.11) \quad \int_{\Omega} u^\varepsilon(x)v(x) \, dx \rightarrow \int_{\Omega} y^0(x)v(x) \, dx \quad \text{as } \varepsilon \rightarrow 0.$$

Consider the normalized characteristic function

$$\bar{\chi}_{\mathcal{V}_\delta(x)}(z) := \begin{cases} \frac{1}{|\mathcal{V}_\delta(x)|}, & z \in \mathcal{V}_\delta(x), \\ 0, & z \notin \mathcal{V}_\delta(x), \end{cases}$$

as the test function in (2.11). Then one obtains the pointwise convergence of averages $(Q_\delta u^\varepsilon)(x) \rightarrow (Q_\delta y^0)(x)$ as $\varepsilon \rightarrow 0$ for $x \in \Omega_\delta$. The L^2 -convergence follows from the uniform estimate of $|(Q_\delta u^\varepsilon)(x)|$ and Lebesgue’s Dominated Convergence Theorem. \square

Since $Y \hookrightarrow H$, for a given $y \in Y$, almost every $x \in \Omega_\delta$ is a Lebesgue point, i.e.,

$$(2.12) \quad \lim_{\delta \rightarrow 0} \frac{1}{|\mathcal{V}_\delta(x)|} \int_{\mathcal{V}_\delta(x)} y(z) \, dz = y(x).$$

For small $\delta > 0$, we consider the following approximation of the above limit:

$$\frac{1}{|\mathcal{V}_\delta(x)|} \int_{\mathcal{V}_\delta(x)} y(z) \, dz \approx \lim_{\delta \rightarrow 0} \frac{1}{|\mathcal{V}_\delta(x)|} \int_{\mathcal{V}_\delta(x)} y(z) \, dz = y(x).$$

Additional integrability of ∇y provides a rate for such an approximation.

LEMMA 2.10. *Suppose that $y \in W^{1,p}(\Omega)$ with $\Omega \subset \mathbb{R}^d$ and $d < p < \infty$. Then*

$$\|y - Q_\delta y\|_{H^\delta} \leq C_p(y) \delta^{\frac{d(p-2)+1}{p}},$$

where the constant $C_p(y) < \infty$ is independent of δ , but it depends on $\|\nabla y\|_{L^p(\Omega)}$.

Proof. First, we use a well-known trick that controls the deviation of a function from its average on convex sets (see e.g. [2, Lemma 4.28]). Let $x \in \Omega_\delta$ and define the convex ball $\mathcal{V}_\delta(x) \subset \Omega$. For $y \in C^1(\bar{\Omega})$, $z \in \mathcal{V}_\delta(x)$ and for all $t \in [0, 1]$, we get

$$y(z) - y(x) = \int_0^1 \frac{d}{dt} y(x + t(z-x)) dt = \int_0^1 \nabla y(x + t(z-x)) \cdot (z-x) dt.$$

Integrating the above equality over $\mathcal{V}_\delta(x)$ and performing the change of variables $\xi = x + t(z-x)$, we obtain

$$(2.13) \quad \left| \int_{\mathcal{V}_\delta(x)} y(z) dz - |\mathcal{V}_\delta(x)| y(x) \right| \leq \int_0^1 \frac{1}{t^d} \int_{\mathcal{V}_{t\delta}(x)} |\nabla y(\xi)| \left| \frac{\xi-x}{t} \right| d\xi dt.$$

Hölder's inequality with $\frac{1}{p} + \frac{1}{q} = 1$, in conjunction with the fact that $\mathcal{V}_{t\delta}(x) \subseteq \mathcal{V}_\delta(x)$, yields the following estimates:

$$\begin{aligned} \int_0^1 \frac{1}{t^{d+1}} \int_{\mathcal{V}_{t\delta}(x)} |\nabla y(\xi)| |\xi - x| d\xi dt &\leq \|\nabla y\|_{L^p(\mathcal{V}_\delta(x))} \int_0^1 \frac{1}{t^{d+1}} \left(\int_{\mathcal{V}_{t\delta}(x)} |\xi - x|^q d\xi \right)^{\frac{1}{q}} dt \\ &\leq \|\nabla y\|_{L^p(\mathcal{V}_\delta(x))} \int_0^1 \frac{dt}{t^{\frac{d}{p}}} \left(\int_{\mathcal{V}_\delta(x)} |x - z|^q dz \right)^{\frac{1}{q}} \leq \frac{\|\nabla y\|_{L^p(\Omega)}}{1 - \frac{d}{p}} \left(\int_{\mathcal{V}_\delta(x)} |x - z|^q dz \right)^{\frac{1}{q}}, \end{aligned}$$

where we used the boundedness of the dt -integral for $\frac{d}{p} < 1$. Since $\rho(r) := \rho(|x - z|) = |x - z|^q$ is radially symmetric on $\mathcal{V}_\delta(x)$, integration in polar coordinates gives:

$$\left(\int_{\mathcal{V}_\delta(x)} |x - z|^q dz \right)^{\frac{1}{q}} = |\mathcal{S}_\delta|^{\frac{1}{q}} \left(\int_0^{\delta/2} \rho(r) r^{d-1} dr \right)^{\frac{1}{q}} = C(d) \delta^{\frac{2d-1+q}{q}},$$

where \mathcal{S}_δ is the $(d-1)$ -sphere of radius $\frac{\delta}{2}$ with $|\mathcal{S}_\delta| = \frac{2\pi^{d/2}}{\Gamma(d/2)} (\delta/2)^{d-1}$, Γ is Euler's gamma function and $C(d) \in \mathbb{R}$ is δ -independent. Dividing (2.13) by $|\mathcal{V}_\delta(x)|$ with $|\mathcal{V}_\delta(x)| = \frac{\pi^{d/2}}{\Gamma(d/2+1)} (\delta/2)^d$, combining the estimates and integrating, we get

$$\left(\int_{\Omega_\delta} |y(x) - (Q_\delta y)(x)|^2 dx \right)^{1/2} \leq C_p(y) \delta^{\frac{d(2-q)+q-1}{q}},$$

where $C_p(y) := C(d, p, \Omega) \|\nabla y\|_{L^p(\Omega)}$. The density of $C^1(\bar{\Omega})$ in $W^{1,p}(\Omega)$ extends the above estimate to the desired result. \square

Under a mild assumption on the regularity of $y^0 \in Y$, we prove the following result.

THEOREM 2.11 (Upscaling consistency). *Suppose that Assumptions 2.6, 2.8 hold, $y^0 \in Y \subset H^2(\Omega)$ with $\Omega \subset \mathbb{R}^d$, $d < p < \infty$ and $d \leq 3$. Then, for $\delta > 0$, it holds:*

$$\lim_{\varepsilon \rightarrow 0} \mathcal{R}_\delta(y(u^\varepsilon), u^\varepsilon) \leq C_p(y^0)^2 \delta^{\frac{2d(p-2)+2}{p}} + 2C_{\mathcal{L}[u]}^2 + |\Omega \setminus \Omega_\delta|^{\frac{2+\gamma}{\gamma}} C_w,$$

where $C_p(y^0) \in \mathbb{R}_+$ and $C_{\mathcal{L}[u]}$ are according to Lemma 2.10 and Assumption 2.8, respectively, and $C_w \in \mathbb{R}_+$ is ε -independent.

Proof. The triangle inequality and Young's inequality yield

$$(2.14) \quad \mathcal{R}_\delta(y(u^\varepsilon), u^\varepsilon) \leq 2\|\bar{Q}_\delta u^\varepsilon - y^0\|_H^2 + 2\|y^0 - y(u^\varepsilon)\|_H^2.$$

Similarly, the estimation of the first term in (2.14) gives

$$(2.15) \quad \|\bar{Q}_\delta u^\varepsilon - y^0\|_H^2 \leq 2\|Q_\delta u^\varepsilon - Q_\delta y^0\|_{H^\delta}^2 + 2\|y^0 - Q_\delta y^0\|_{H^\delta}^2 + \|u^\varepsilon - y^0\|_{L^2(\Omega \setminus \Omega_\delta)}^2.$$

Clearly, Assumption 2.6 implies that $u^\varepsilon \rightharpoonup y^0$ as $\varepsilon \rightarrow 0$ in H . Thus, Lemma 2.9 guarantees that the first term on the right-hand side of (2.15) vanishes as $\varepsilon \rightarrow 0$. Since $\nabla y^0 \in H^1(\Omega)$ due to $Y \subset H^2(\Omega)$ and $d \leq 3$, the Sobolev embedding yields $\|\nabla y^0\|_{L^p(\Omega)} < \infty$ for $p \leq 6$. Observe further that y^0 is ε -independent, hence $C_p(y^0)$ is also ε -independent. Therefore, Lemma 2.10 guarantees that $\|y^0 - Q_\delta y^0\|_{H^\delta}^2 \leq C_p(y^0)^2 \delta^{\frac{2d(p-2)+2}{p}}$ and the latter estimate holds in the limit $\varepsilon \rightarrow 0$.

We estimate the second term in (2.14) by appealing to Assumption 2.8. Next, let $s = \frac{2+\gamma}{2}$ and $r = \frac{2+\gamma}{\gamma}$. Then $\frac{1}{s} + \frac{1}{r} = 1$ and the Hölder estimate holds

$$\|u^\varepsilon - y^0\|_{L^2(\Omega \setminus \Omega_\delta)}^2 \leq |\Omega \setminus \Omega_\delta|^{\frac{2+\gamma}{\gamma}} \|u^\varepsilon - y^0\|_{L^{2+\gamma}(\Omega)}^2$$

for the third term in (2.15). The uniform boundedness of $\{u^\varepsilon\}$ implies the existence of $C_w \in \mathbb{R}_+$ such that $\|u^\varepsilon - y^0\|_{L^{2+\gamma}(\Omega)}^2 \leq C_w$, hence completing the proof. \square

Suppose that $\nabla y^0 \notin L^p(\Omega)$ for some $p > d$. Then Lemma 2.10 is not applicable. In this case, the coupling term (2.10) can be modified as follows:

$$(2.16) \quad \mathcal{R}_\delta(y(u^\varepsilon), u^\varepsilon) := \|\bar{Q}_\delta u^\varepsilon - \bar{Q}_\delta y(u^\varepsilon)\|_H^2.$$

Then, Theorem 2.11 still holds with $C_p(y^0) = 0$.

3. Learning-informed PDE-constrained optimization. We cast our hybrid physics-informed neural network based multiscale approach for a fixed $\varepsilon > 0$ into the following learning-informed PDE-constrained optimization problem:

$$(3.1) \quad \begin{cases} \inf J(y, v_{\theta, n}) := \mathcal{J}(v_{\theta, n}) + \tau_2 \mathcal{R}_\delta(y, v_{\theta, n}) \text{ over } (y, v_{\theta, n}) \in Y \times B_{\bar{r}^\varepsilon, \theta, n}(u^\varepsilon), \\ \text{s.t. } e(y, v_{\theta, n}) = 0, \end{cases}$$

where $B_{\bar{r}^\varepsilon, \theta, n}(u^\varepsilon) := B_{\bar{r}^\varepsilon}(u^\varepsilon) \cap \mathfrak{N}_{\theta, n}$ with $u^\varepsilon, \bar{r}^\varepsilon$ according to Assumption 2.4, $J : Y \times U \rightarrow \mathbb{R}_{\geq 0}$ and fixed $\tau_2, \delta \in \mathbb{R}_{\geq 0}$. Further, let $e : Y \times U \rightarrow Y^*$ be given by $e : (w, v) \mapsto e(w, v) := b_{\mathcal{L}}[v](w, \cdot) - \langle f, \cdot \rangle_{Y^*, Y}$ and \mathcal{R}_δ denote the coupling term in (2.16). Note that for u^ε according to Assumption 2.4 there exists $v \in X$ arbitrarily close to u^ε due to the density of the embedding $X \hookrightarrow U$. Then, Assumption 2.5 implies the existence of $\theta \in \mathbb{R}^{N_{n_\varepsilon^*}}$ such that

$$\|u^\varepsilon - v_{\theta, n_\varepsilon^*}\|_U \leq \|u^\varepsilon - v\|_U + C\|v - v_{\theta, n_\varepsilon^*}\|_X \leq \bar{r}^\varepsilon,$$

for sufficiently large $n_\varepsilon^* \in \mathbb{N}$. Then, for all $n \geq n_\varepsilon^*$, $B_{\bar{r}^\varepsilon, \theta, n}(u^\varepsilon) \neq \emptyset$ and the following *fine-to-coarse scale map* is well-defined:

$$(3.2) \quad S : B_{\bar{r}^\varepsilon, \theta, n}(u^\varepsilon) \subset U \rightarrow Y, \quad u \mapsto y(u) := S(u),$$

with $e(y(u), u) = 0$. Note that since (2.7) is non-convex in general, finding θ with $v_{\theta, n} \in B_{\bar{r}^\varepsilon, \theta, n}(u^\varepsilon)$ requires solving an associated non-convex optimization problem. In practice, however, the latter can often not be guaranteed.

We also need the following.

ASSUMPTION 3.1 (Continuity). *Let $u^\varepsilon \in U$ be the solution of (2.1) and $\{u_k^\varepsilon\} \subset B_{\bar{r}^\varepsilon}(u^\varepsilon) \cap X$ its approximating sequence. Then $S(u_k^\varepsilon) \rightarrow S(u^\varepsilon)$ in Y as $k \rightarrow \infty$.*

Eliminating y from the set of independent variables in (3.1) results in the reduced optimization problem

$$(3.3) \quad \inf \widehat{J}(v_{\theta, n}) := J(S(v_{\theta, n}), v_{\theta, n}) \text{ over } v_{\theta, n} \in B_{\bar{r}^\varepsilon, \theta, n}(u^\varepsilon).$$

We note that guaranteeing the existence of minimizers in $\mathfrak{N}_{\theta, n}$ for (3.3) is not possible, in general, as $\mathfrak{N}_{\theta, n}$ may not be topologically closed in U . In order to cope with this, we resort to the notion of quasi-minimization; cf. [57], see also [10]. The latter only requires the existence of an infimum of \widehat{J} over $B_{\bar{r}^\varepsilon, \theta, n}(u^\varepsilon) \neq \emptyset$.

Clearly, since $\widehat{J}(\cdot) \geq 0$, $\inf \widehat{J}$ exists over $B_{\bar{r}^\varepsilon, \theta, n}(u^\varepsilon)$ for every $n \geq n_\varepsilon^*$. Now let $\{\gamma_n\}_{n \geq n_\varepsilon^*}$ be a real sequence with $\gamma_n > 0$ for all $n \geq n_\varepsilon^*$ and $\gamma_n \downarrow 0$ as $n \rightarrow \infty$. Then, for every $n \geq n_\varepsilon^*$, there exists $u_{\hat{\theta}, n}^\varepsilon \in B_{\bar{r}^\varepsilon, \theta, n}(u^\varepsilon)$ such that

$$\widehat{J}(u_{\hat{\theta}, n}^\varepsilon) \leq \inf_{v_{\theta, n} \in B_{\bar{r}^\varepsilon, \theta, n}(u^\varepsilon)} \widehat{J}(v_{\theta, n}) + \gamma_n.$$

We refer to $\{u_{\hat{\theta}, n}^\varepsilon\}_{n \geq n_\varepsilon^*}$ as a sequence of quasi-minimizers of (3.3). In the following result, we consider J with the coupling term (2.16), but extending it to (2.10) is straightforward.

THEOREM 3.2. *Suppose that Assumptions 2.4, 2.3, 2.5, and 3.1 hold. Let $\{u_{\theta,n}^\varepsilon\}_{n \geq n_\varepsilon^*}$, $v_{\theta,n}^\varepsilon \in B_{\bar{r}^\varepsilon, \theta, n}(u^\varepsilon)$ be a quasi-minimizing sequence for $\widehat{J} : U \rightarrow \mathbb{R}_{\geq 0}$, where $B_{\bar{r}^\varepsilon}(u^\varepsilon)$ is chosen according to Assumption 2.4 and $n_\varepsilon^* \in \mathbb{N}$ is chosen according to Assumption 2.5 to guarantee that $B_{\bar{r}^\varepsilon, \theta, n}(u^\varepsilon) \neq \emptyset$ for all $n \geq n_\varepsilon^*$. Then, $\lim_{n \rightarrow \infty} \widehat{J}(u_{\theta,n}^\varepsilon) \leq \tau_2 \mathcal{R}_\delta(y(u^\varepsilon), u^\varepsilon)$, where u^ε is the solution to (2.1) according to Assumption 2.1. Moreover, for $\tau_1 \geq 1$ it holds that*

$$(3.4) \quad \lim_{n \rightarrow \infty} \|u_{\theta,n}^\varepsilon - u^\varepsilon\|_V \leq \frac{1}{\sqrt{C_s^\varepsilon}} \sqrt{\tau_2 \mathcal{R}_\delta(y(u^\varepsilon), u^\varepsilon)}.$$

Proof. Let u^ε be the solution to (2.1) and $\{u_k^\varepsilon\}$, $u_k^\varepsilon \in X$ for all k , be its approximating sequence (2.2). Let $\{r_k\}$ be a positive real sequence with $r_k \downarrow 0$ monotonically as $k \rightarrow \infty$ and choose $K_\varepsilon \in \mathbb{N}$ sufficiently large such that $B_{r_k}(u_k^\varepsilon) := \{v \in U : \|u_k^\varepsilon - v\|_U \leq r_k\} \subset B_{\bar{r}^\varepsilon}(u^\varepsilon)$ for all $k \geq K_\varepsilon$. Assumption 2.5 and the dense embedding $X \hookrightarrow U$ imply that $\|u_k^\varepsilon - v_{\theta, n_k}^\varepsilon\|_U \leq C \|u_k^\varepsilon - v_{\theta, n_k}^\varepsilon\|_X \leq C \epsilon_{n_k} \leq r_k$ for $k \geq K_\varepsilon$ and some $v_{\theta, n_k}^\varepsilon \in \mathfrak{N}_{\theta, n_k}$, where $n_k := n(k) \in \mathbb{N}$, $\epsilon_{n_k} \in \mathbb{R}_+$ and $C > 0$ is some embedding constant. Observe further that $B_{r_k}(u_k^\varepsilon) \subset B_{\bar{r}^\varepsilon}(u^\varepsilon)$ for $k \geq K_\varepsilon$ implies $\epsilon_{n_{K_\varepsilon}} \leq \epsilon_{n_\varepsilon^*}$. Therefore, $n_{K_\varepsilon} \geq n_\varepsilon^*$ with $\mathfrak{N}_{\theta, n_\varepsilon^*} \subseteq \mathfrak{N}_{\theta, n_{K_\varepsilon}}$ holds and there exists a sequence $\{v_{\theta, n_k}^\varepsilon\}_{k \geq K_\varepsilon}$ with $v_{\theta, n_k}^\varepsilon \in B_{r_k, \theta, n_k}(u_k^\varepsilon) \subset B_{\bar{r}^\varepsilon}(u^\varepsilon)$. We note that Assumption 2.5 implies that $\{\epsilon_{n_k}\}_{k \geq K_\varepsilon}$ converges to 0 as $k \rightarrow \infty$, thus $n_k \rightarrow \infty$ as $k \rightarrow \infty$. Then, once again the embedding $X \hookrightarrow U$ implies that

$$\|u^\varepsilon - v_{\theta, n_k}^\varepsilon\|_U \leq \|u^\varepsilon - u_k^\varepsilon\|_U + C \|u_k^\varepsilon - v_{\theta, n_k}^\varepsilon\|_X \rightarrow 0 \quad \text{as } k \rightarrow \infty.$$

In addition, the boundedness of \mathcal{A}^ε and \mathcal{B} , respectively, and the upper bound in (2.3) result in the existence of $C^\varepsilon \in \mathbb{R}_+$, possibly dependent on ε , such that

$$\|\mathcal{A}^\varepsilon v_{\theta, n_k}^\varepsilon - f\|_H + \|\mathcal{B} v_{\theta, n_k}^\varepsilon\|_Z \leq C^\varepsilon \|v_{\theta, n_k}^\varepsilon - u_k^\varepsilon\|_X + \|\mathcal{A}^\varepsilon u_k^\varepsilon - f\|_H + \|\mathcal{B} u_k^\varepsilon\|_Z \rightarrow 0$$

as $k \rightarrow 0$. Therefore, $\{v_{\theta, n_k}^\varepsilon\}_{k \geq K_\varepsilon}$ is also an approximating sequence (2.2).

Next, we study the coupling term and show that

$$(3.5) \quad \lim_{k \rightarrow \infty} \mathcal{R}_\delta(S(v_{\theta, n_k}^\varepsilon), v_{\theta, n_k}^\varepsilon) \leq \mathcal{R}_\delta(y(u^\varepsilon), u^\varepsilon).$$

Indeed, invoking the triangle inequality and $\bar{Q}_\delta \in L(H)$, we get

$$(3.6) \quad \begin{aligned} \mathcal{R}_\delta(S(v_{\theta, n_k}^\varepsilon), v_{\theta, n_k}^\varepsilon) &\leq \|\bar{Q}_\delta\|^2 \|v_{\theta, n_k}^\varepsilon - u_k^\varepsilon\|_H^2 + \|\bar{Q}_\delta u_k^\varepsilon - \bar{Q}_\delta y(v_{\theta, n_k}^\varepsilon)\|_H^2 \\ &\quad + 2\|\bar{Q}_\delta\| \|v_{\theta, n_k}^\varepsilon - u_k^\varepsilon\|_H \|\bar{Q}_\delta u_k^\varepsilon - \bar{Q}_\delta y(v_{\theta, n_k}^\varepsilon)\|_H. \end{aligned}$$

Since $v_{\theta, n_k}^\varepsilon \in B_{\bar{r}^\varepsilon, \theta, n_\varepsilon^*}(u^\varepsilon)$ for $k \geq K_\varepsilon$, the fine-to-coarse mapping (3.2) is well-defined in (3.6). The embedding $U \hookrightarrow H$ guarantees that the first and the last term in (3.6) vanish as $k \rightarrow 0$. Similarly, one estimates the intermediate term in (3.6):

$$(3.7) \quad \begin{aligned} \|\bar{Q}_\delta u_k^\varepsilon - \bar{Q}_\delta y(v_{\theta, n_k}^\varepsilon)\|_H^2 &\leq \mathcal{R}_\delta(y(u^\varepsilon), u_k^\varepsilon) + \|\bar{Q}_\delta\|^2 \|y(u^\varepsilon) - y(v_{\theta, n_k}^\varepsilon)\|_H^2 \\ &\quad + 2\|\bar{Q}_\delta\| \|\bar{Q}_\delta u_k^\varepsilon - \bar{Q}_\delta y(u^\varepsilon)\|_H \|y(u^\varepsilon) - y(v_{\theta, n_k}^\varepsilon)\|_H. \end{aligned}$$

We use Assumption 3.1 and the compactness of $Y \hookrightarrow H$ to obtain $\lim_{k \rightarrow \infty} \|y(v_{\theta, n_k}^\varepsilon) - y(u^\varepsilon)\|_H^2 = 0$. Therefore, (3.5) readily follows from (3.6) and (3.7).

Next, we study the limit $\lim_{n \rightarrow \infty} \widehat{J}(u_{\theta, n}^\varepsilon)$. The stability bound (2.3) gives

$$(3.8) \quad \mathcal{J}(v_{\theta, n_k}^\varepsilon) \leq (\|f - \mathcal{A}^\varepsilon u_k^\varepsilon\|_H + C_b^\varepsilon r_k)^2 + \tau_1 (\|\mathcal{B} u_k^\varepsilon\|_Z + C_b^\varepsilon r_k)^2.$$

Since $B_{\bar{r}^\varepsilon, \theta, n_{K_\varepsilon}}(u^\varepsilon) \neq \emptyset$ and $B_{\bar{r}^\varepsilon, \theta, n_{K_\varepsilon}}(u^\varepsilon) \subset B_{\bar{r}^\varepsilon}(u^\varepsilon)$, we can find a quasi-minimizer $u_{\theta, n_k}^\varepsilon \in B_{\bar{r}^\varepsilon, \theta, n_k}(u^\varepsilon)$ for each $k \geq K_\varepsilon$ with $\gamma_{n_k} > 0$ and $\gamma_{n_k} \downarrow 0$ such that

$$(3.9) \quad \widehat{J}(u_{\theta, n_k}^\varepsilon) \leq \inf_{v \in B_{\bar{r}^\varepsilon, \theta, n_k}(u^\varepsilon)} \widehat{J}(v) + \gamma_{n_k} \leq \widehat{J}(v_{\theta, n_k}^\varepsilon) + \gamma_{n_k}.$$

Then, it follows from (3.5) and (3.8) that $\lim_{k \rightarrow \infty} \widehat{J}(v_{\theta, n_k}^\varepsilon) \leq \tau_2 \mathcal{R}_\delta(y(u^\varepsilon), u^\varepsilon)$. Hence, for any $\epsilon_J > 0$, there exists $K_{\epsilon_J} \geq K_\varepsilon$ such that $\widehat{J}(u_{\theta, n_k}^\varepsilon) \leq \epsilon_J/2 + \tau_2 \mathcal{R}_\delta(y(u^\varepsilon), u^\varepsilon)$ for all $k \geq K_{\epsilon_J}$. By resorting to the notion of a quasi-minimizing sequence $\{u_{\theta, n}^\varepsilon\}_{n \geq n_\varepsilon^*}$, the existence of $N_{\epsilon_J} \geq n_\varepsilon^*$ follows with $\gamma_n \leq \epsilon_J/2$ for all $n \geq N_{\epsilon_J}$. For $\tilde{N}_{\epsilon_J} = \max\{n_{K_{\epsilon_J}}, N_{\epsilon_J}\}$ and $n \geq \tilde{N}_{\epsilon_J}$, we have $\mathfrak{N}_{\theta, \tilde{N}_{\epsilon_J}} \subseteq \mathfrak{N}_{\theta, n}$, and

$$\widehat{J}(u_{\theta, n}^\varepsilon) \leq \inf_{v \in B_{\bar{r}^\varepsilon, \theta, n}(u^\varepsilon)} \widehat{J}(v) + \gamma_n \leq \widehat{J}(u_{\theta, \tilde{N}_{\epsilon_J}}^\varepsilon) + \gamma_n \leq \epsilon_J + \tau_2 \mathcal{R}_\delta(y(u^\varepsilon), u^\varepsilon).$$

Since ϵ_J was arbitrarily chosen, the first limit claim is shown.

The stability estimate (2.3) and $\tau_1 \geq 1$ imply that

$$C_s^\varepsilon \|u_{\theta, n}^\varepsilon - u^\varepsilon\|_V^2 \leq \|\mathcal{A}^\varepsilon u_{\theta, n}^\varepsilon - \mathcal{A}^\varepsilon u^\varepsilon\|_H^2 + \tau_1 \|\mathcal{B} u_{\theta, n}^\varepsilon - \mathcal{B} u^\varepsilon\|_Z^2 \leq \widehat{J}(u_{\theta, n}^\varepsilon).$$

Then, (3.4) follows from the previous result and the a-posteriori bound above. \square

In our setting, \mathcal{R}_δ serves the purpose of a regularizer in the training process, and one might expect from Theorem 2.11 and Theorem 3.2 that its efficiency increases with decreasing ε . However, it may happen that $C_s^\varepsilon \rightarrow 0$ as $\varepsilon \rightarrow 0$ for the standard $H = L^2(\Omega)$ PINN objective, making the bound (3.4) merely of qualitative nature.

REMARK 3.3. *In general, $\inf \widehat{J}$ and $\inf \mathcal{J}$ over $B_{\bar{r}^\varepsilon, \theta, n}(u^\varepsilon)$ are different. Therefore, quasi-minimizers of \widehat{J} and \mathcal{J} are also different. For a quasi-minimizing sequence $\{u_{\theta, n}^\varepsilon\}_{n \in \mathbb{N}}$ of \mathcal{J} , it holds that $\|u_{\theta, n}^\varepsilon - u^\varepsilon\|_V \leq \frac{1}{\sqrt{C_s^\varepsilon}} \sqrt{\mathcal{J}(u_{\theta, n}^\varepsilon)}$ with $\lim_{n \rightarrow \infty} \mathcal{J}(u_{\theta, n}^\varepsilon) = 0$; cf. [57, Proposition 3.1 and Theorem 3.2].*

3.1. Discrete approximation. The (fully) discrete version of (3.1) comes in three steps: (i) First, we consider $\theta \rightarrow v_{\theta, n}$, reducing every NN-function to its finite set of generating parameters belonging to \mathbb{R}^{N_n} ; (ii) then, we replace the state y by a finite dimensional approximation y_h , with h indicating the associated discretization parameter such as, e.g., the mesh width in a finite element method [9]; (iii) finally, the discrete version \widehat{J} of \mathcal{J} is replaced by its quadrature approximation $\widehat{J}_D^{M, h}$, where M indicates the number of collocation or quadrature points, and D is related to a discretization of the compression operator (2.9).

Let us start with (i) and define

$$(3.10) \quad \mathcal{S} := S \circ \mathfrak{F}_n : \mathbb{R}^{N_n} \rightarrow Y, \quad \theta \mapsto y(v_{\theta, n}) := \mathcal{S}(\theta),$$

$$(3.11) \quad \widehat{\mathcal{J}} := \widehat{J} \circ \mathfrak{F}_n : \mathbb{R}^{N_n} \rightarrow \mathbb{R}_{\geq 0}, \quad \theta \mapsto \widehat{\mathcal{J}}(\theta) := J(\mathcal{S}(\theta), \mathfrak{F}_n(\theta)),$$

where \mathfrak{F}_n is according to (2.7). We invoke the following assumption on differentiability.

ASSUMPTION 3.4 (Fréchet differentiability). *The fine-to-coarse scale map (3.2) is continuously Fréchet differentiable and $\mathfrak{F}_n \in C^\infty(\mathbb{R}^{N_n}, X)$.*

Assumption 3.4 and the chain rule imply that \mathcal{S} is continuously Fréchet differentiable. We also note that \mathfrak{F}_n satisfies Assumption 3.4 for smooth activation functions in

a neural network, i.e., $\sigma \in C^\infty(\mathbb{R})$. Accordingly, the differentiability requirement can be reduced via reducing the one on σ . Via the implicit function theorem for $e(y(v_{\theta,n}), \mathfrak{F}_n(\theta)) = 0$ we obtain

$$(3.12) \quad e_y(y(v_{\theta,n}), \theta) \mathcal{S}'(\theta) + e_v(y(v_{\theta,n}), \mathfrak{F}_n(\theta)) \mathfrak{F}'_n(\theta) = 0,$$

where we have $\mathcal{S}'(\theta) = S'(\mathfrak{F}_n(\theta)) \mathfrak{F}'_n(\theta) \in L(\mathbb{R}^{N_n}, Y)$ and, upon obvious identification, $\mathcal{S}'(\theta)^* \in L(Y^*, \mathbb{R}^{N_n})$.

By applying the chain rule, we find the gradient of (3.11):

$$(3.13) \quad \nabla \widehat{\mathfrak{J}}(\theta) = \mathcal{S}'(\theta)^* \partial_y J(y(v_{\theta,n}), \mathfrak{F}_n(\theta)) + \mathfrak{F}'_n(\theta)^* \partial_v J(y(v_{\theta,n}), \mathfrak{F}_n(\theta)),$$

In practical realizations of PINNs, the second summand in (3.13) is typically produced by automatic differentiation, and the first summand is realized via the adjoint method [31]. For the latter, we need the bilinear form $b_{\mathcal{L}^*}[v_{\theta,n}](\cdot, \cdot) : Y \times Y \rightarrow \mathbb{R}$ with

$$(3.14) \quad b_{\mathcal{L}^*}[v_{\theta,n}](w, v) := \langle e_y(y(v_{\theta,n}), \mathfrak{F}_n(\theta))^* w, v \rangle_{Y^*, Y}.$$

The following guarantees that (3.14) is well-defined.

ASSUMPTION 3.5. *Suppose that $B_{\bar{r}^\varepsilon, \theta, n_\varepsilon^*}(u^\varepsilon) \subset U$, where $\bar{r}^\varepsilon \in \mathbb{R}_+$ is according to Assumption 2.4 and n_ε^* is chosen sufficiently large as in Assumption 2.5. Then, there exist $C_{b^*}^\varepsilon, C_{c^*}^\varepsilon \in \mathbb{R}_+$ such that for all $v_{\theta,n} \in B_{\bar{r}, \theta, n}(u^\varepsilon)$ with $n \geq n_\varepsilon^*$ it holds that*

$$(3.15) \quad b_{\mathcal{L}^*}[v_{\theta,n}](v, w) \leq C_{b^*}^\varepsilon \|v\|_Y \|w\|_Y, \text{ and } b_{\mathcal{L}^*}[v_{\theta,n}](v, v) \geq C_{c^*}^\varepsilon \|v\|_Y^2, \quad \forall v, w \in Y.$$

Note that Assumption 3.5 and (3.12) yield the adjoint equation

$$e_y(y(v_{\theta,n}), \mathfrak{F}_n(\theta))^* p(v_{\theta,n}) = -\partial_y J(y(v_{\theta,n}), \mathfrak{F}_n(\theta)) = 2\tau_2 \bar{Q}_\delta^* (\bar{Q}_\delta v_{\theta,n} - \bar{Q}_\delta y(v_{\theta,n})),$$

or its counterpart in weak form:

$$(3.16) \quad b_{\mathcal{L}^*}[v_{\theta,n}](p(v_{\theta,n}), v) = 2\tau_2 (\bar{Q}_\delta v_{\theta,n} - \bar{Q}_\delta y(v_{\theta,n}), \bar{Q}_\delta v)_H \quad \forall v \in Y,$$

where $p(v_{\theta,n}) := p(y(v_{\theta,n})) \in Y$ denotes the adjoint variable (or adjoint state, sometimes also called co-state).

Now we come to the second step of discretization. Here we use the finite element (FE) method applied to the coarse-scale equation. More specifically, let $Y_h := \text{span}\{\phi_j, 1 \leq j \leq N_h\} \subset Y$, $N_h \in \mathbb{N}$, be the standard finite dimensional space of piecewise-linear and globally continuous functions over a domain $\Omega \subset \mathbb{R}^d$. Of course, other choices of Y_h are possible as well [9]. The finite element approximation of (2.6), which involves the neural network based function $v_{\theta,n}$ as data, is then obtained by a standard Galerkin projection: Find $y_h(v_{\theta,n}) \in Y_h$ such that

$$(3.17) \quad b_{\mathcal{L}^*}[v_{\theta,n}](y_h(v_{\theta,n}), v_h) = \langle \tilde{f}, v_h \rangle_{Y^*, Y} \quad \forall v_h \in Y_h.$$

Assumption 2.4 and Assumption 2.5 imply that (3.17) admits a unique solution $y_h(v_{\theta,n}) \in Y_h$ for all $v_{\theta,n} \in B_{\bar{r}^\varepsilon, \theta, n}(u^\varepsilon)$ with $n \geq n_\varepsilon^*$.

The adjoint equation is discretized similarly: Find $p_h(v_{\theta,n}) := p_h(y_h(v_{\theta,n})) \in Y_h$ such that

$$(3.18) \quad b_{\mathcal{L}^*}[v_{\theta,n}](p_h(v_{\theta,n}), v_h) = 2\tau_2 (\bar{Q}_\delta v_{\theta,n} - \bar{Q}_\delta y_h(v_{\theta,n}), \bar{Q}_\delta v_h)_H \quad \forall v_h \in Y_h.$$

Assumption 3.5 implies that (3.18) admits a unique solution $p_h(v_{\theta,n}) \in Y_h$ for $v_{\theta,n} \in B_{\bar{r}^\varepsilon, \theta, n}(u^\varepsilon)$.

Regarding both of the above equations the following error estimates hold true.

THEOREM 3.6. *Suppose that Assumptions 2.3, 2.4, 2.5, 3.1 and 3.5 hold. Furthermore, let $Y \subset H^2(\Omega)$ and for all $u_1, u_2 \in B_{\bar{r}\varepsilon}(u^\varepsilon)$ and $v, w \in Y$ it holds that*

$$(3.19) \quad |b_{\mathcal{L}}[u_1](v, w) - b_{\mathcal{L}}[u_2](v, w)| \leq C^\varepsilon \|u_1 - u_2\|_V \|v\|_Y \|w\|_Y,$$

where $C^\varepsilon \in \mathbb{R}_+$. In addition, (3.19) holds also for the adjoint form $b_{\mathcal{L}^*}[u](\cdot, \cdot)$. Then

$$(3.20) \quad \lim_{h \rightarrow 0} \lim_{n \rightarrow \infty} \|y(u^\varepsilon) - y_h(u_{\theta, n}^\varepsilon)\|_Y \leq C_y^\varepsilon \sqrt{\tau_2 \mathcal{R}_\delta(y(u^\varepsilon), u^\varepsilon)},$$

$$(3.21) \quad \lim_{h \rightarrow 0} \lim_{n \rightarrow \infty} \|p(u^\varepsilon) - p_h(u_{\theta, n}^\varepsilon)\|_Y \leq C_{ad}^\varepsilon \sqrt{\tau_2 \mathcal{R}_\delta(y(u^\varepsilon), u^\varepsilon)},$$

where $p(u^\varepsilon) := p(y(u^\varepsilon)) \in Y$, $p_h(u_{\theta, n}^\varepsilon) := p_h(y_h(u_{\theta, n}^\varepsilon)) \in Y_h$, $C_y^\varepsilon, C_{ad}^\varepsilon \in \mathbb{R}_+$, and the latter constants may depend on ε .

Proof. For $u_{\theta, n}^\varepsilon \in B_{\bar{r}\varepsilon, \theta, n}(u^\varepsilon)$, we treat $b_{\mathcal{L}}[u_{\theta, n}^\varepsilon](\cdot, \cdot)$ as an approximation of $b_{\mathcal{L}}[u^\varepsilon](\cdot, \cdot)$ and apply Strang's lemma [3, Lemma 2.27] to get the estimate

$$(3.22) \quad \|y(u^\varepsilon) - y_h(u_{\theta, n}^\varepsilon)\|_Y \leq e_{n, h}^{y, rhs} + \inf_{v_h \in Y_h} \left(\left(1 + \frac{C_b^\varepsilon}{C_c^\varepsilon}\right) \|y(u^\varepsilon) - v_h\|_Y \right. \\ \left. + \frac{1}{C_c^\varepsilon} \sup_{w_h \in Y_h} \frac{|b_{\mathcal{L}}[u^\varepsilon](v_h, w_h) - b_{\mathcal{L}}[u_{\theta, n}^\varepsilon](v_h, w_h)|}{\|w_h\|_Y} \right),$$

where $e_{n, h}^{y, rhs}$ represents a discrepancy measure between the right-hand sides of (2.6) and (3.17), but $e_{n, h}^{y, rhs} = 0$ in our case. Let $\mathcal{I}_h y(u^\varepsilon)$ be the interpolant of $y(u^\varepsilon)$ in Y_h . Since $Y \subset H^2(\Omega)$, a well-known [9] interpolation bound yields

$$\inf_{v_h \in Y_h} \|y(u^\varepsilon) - v_h\|_Y \leq \|y(u^\varepsilon) - \mathcal{I}_h y(u^\varepsilon)\|_Y \leq Ch \|y(u^\varepsilon)\|_{H^2(\Omega)} \rightarrow 0 \quad \text{as } h \rightarrow 0.$$

Assumption 2.4 and the boundedness of $\mathcal{I}_h : Y \rightarrow Y_h$ imply that $\|\mathcal{I}_h y(u^\varepsilon)\|_Y \leq C$, where $C \in \mathbb{R}_+$ does not depend on h . Invoking (3.19) and (3.4), we get

$$|b_{\mathcal{L}}[u^\varepsilon](\mathcal{I}_h y(u^\varepsilon), w_h) - b_{\mathcal{L}}[u_{\theta, n}^\varepsilon](\mathcal{I}_h y(u^\varepsilon), w_h)| \leq \frac{C}{\sqrt{C_s^\varepsilon}} \sqrt{\tau_2 \mathcal{R}_\delta(y(u^\varepsilon), u^\varepsilon)} \|w_h\|_Y$$

for $n \rightarrow \infty$. The result (3.20) then follows from (3.22) and the above estimates.

The analysis of the adjoint equation is similar to that of the state equation. However, the discrepancy between the right-hand sides of (3.16) and (3.18), i.e., the quantity

$$e_{n, h}^{p, rhs} := \sup_{v_h \in Y_h} \frac{|2\tau_2 \langle \bar{Q}_\delta(u^\varepsilon - u_{\theta, n}^\varepsilon + y_h(u_{\theta, n}^\varepsilon) - y(u^\varepsilon)), \bar{Q}_\delta v_h \rangle_H|}{\|v_h\|_Y}.$$

needs to be additionally estimated for the application of Strang's lemma. The Cauchy-Schwarz and triangle inequalities, the embeddings $Y \hookrightarrow H$, $V \hookrightarrow H$, and $\bar{Q}_\delta \in L(H)$ yield $C \in \mathbb{R}_+$ such that

$$e_{n, h}^{p, rhs} \leq C \left(\|u^\varepsilon - u_{\theta, n}^\varepsilon\|_V + \|y(u^\varepsilon) - y_h(u_{\theta, n}^\varepsilon)\|_Y \right).$$

Then, the result (3.21) follows from (3.4) and (3.20). \square

Both FE discretized equations result in the following algebraic system:

$$(3.23) \quad \mathbb{B}_h[\boldsymbol{\theta}]\mathbf{y}_h = \mathbb{F}_h, \quad \mathbb{B}_h[\boldsymbol{\theta}]^\top \mathbf{p}_h = 2\tau_2(\mathbb{P}_h[\boldsymbol{\theta}] - \mathbb{P}_h[\mathbf{y}_h]),$$

where $\mathbf{y}_h \in \mathbb{R}^{N_h}$ and $\mathbf{p}_h \in \mathbb{R}^{N_h}$ are the coefficients of the FE functions $y_h = \sum_{i=1}^{N_h} (\mathbf{y}_h)_i \phi_i$ and $p_h = \sum_{i=1}^{N_h} (\mathbf{p}_h)_i \phi_i$. Moreover, $\mathbb{B}_h[\boldsymbol{\theta}] \in \mathbb{R}^{N_h \times N_h}$, $(\mathbb{B}_h[\boldsymbol{\theta}])_{ij} := b_{\mathcal{L}}[v_{\boldsymbol{\theta},n}](\phi_i, \phi_j)$, $\mathbb{F}_h \in \mathbb{R}^{N_h}$, $(\mathbb{F}_h)_j := \langle \tilde{f}, \phi_j \rangle_{Y^*, Y}$ and $\mathbb{P}_h[\boldsymbol{\theta}] \in \mathbb{R}^{N_h}$, $(\mathbb{P}_h[\boldsymbol{\theta}])_j := \langle \bar{Q}_\delta v_{\boldsymbol{\theta},n}, \bar{Q}_\delta \phi_j \rangle_H$.

For item (iii) we assume that $H = L^2(\Omega)$, $Z = L^2(\partial\Omega)$, and apply a Monte-Carlo approach to approximate the integrals in the PINN objective as follows:

$$(3.24) \quad \mathcal{J}^M(v_{\boldsymbol{\theta},n}^M) := \frac{|\Omega|}{M_\Omega} \sum_{i=1}^{M_\Omega} (\mathcal{A}^\varepsilon v_{\boldsymbol{\theta},n}^M(x_i^r) - f^\varepsilon(x_i^r))^2 + \frac{\tau_1 |\partial\Omega|}{M_{\partial\Omega}} \sum_{i=1}^{M_{\partial\Omega}} (\mathcal{B} v_{\boldsymbol{\theta},n}^M(x_i^b))^2,$$

where $\{x_i^r\}_{i=1}^{M_\Omega}$ and $\{x_i^b\}_{i=1}^{M_{\partial\Omega}}$ are (uniformly random) collocation points in Ω and on $\partial\Omega$, respectively. Assuming that $M := M_\Omega + M_{\partial\Omega}$ is sufficiently large to guarantee that $v_{\boldsymbol{\theta},n}^M \in B_{\tilde{r}^\varepsilon, \boldsymbol{\theta}, n}(u^\varepsilon)$ for all $n \geq n_\varepsilon^*$, we discretize (2.16) using a quadrature rule:

$$(3.25) \quad \mathcal{R}_{\delta, D}^h(y_h(v_{\boldsymbol{\theta},n}^M), v_{\boldsymbol{\theta},n}^M) := \sum_{i=1}^{N_h} w_i^h ((\bar{Q}_\delta^D v_{\boldsymbol{\theta},n}^M)(x_i^h) - (\bar{Q}_\delta^D y_h(v_{\boldsymbol{\theta},n}^M))(x_i^h))^2,$$

where $\{x_i^h, w_i^h\}_{i=1}^{N_h}$ are our finite element nodes and quadrature weights, and

$$(3.26) \quad (\bar{Q}_\delta^D v)(x_i^h) = \begin{cases} \frac{1}{|\mathcal{V}_\delta^D(x_i^h)|} \sum_{x_j^h \in \mathcal{V}_\delta^D(x_i^h)} v(x_j^h), & x_i^h \in \Omega_\delta, \\ v(x_i^h), & x_i^h \in \Omega \setminus \Omega_\delta, \end{cases}$$

where $v \in C(\bar{\Omega})$ is a continuous function, $\mathcal{V}_\delta^D(x_i^h) := \{x_j^r : |x_j^r - x_i^h| \leq \frac{\delta}{2}\}$ corresponds to the set of residual collocation points around the coarse-scale mesh nodes, and M_D is an associated number of such collocation points. We note that using (2.10) allows us not to apply \bar{Q}_δ^D to the coarse-scale approximation in (3.25), yielding a simple implementation. The discrete components (3.24), (3.25) and (3.26), as well as the mapping (3.10), finally yield the approximation $\widehat{\mathfrak{J}}_D^{M,h}$ of $\widehat{\mathfrak{J}}$.

Algorithmically and assuming that $\nabla \widehat{\mathfrak{J}}_D^{M,h}(\boldsymbol{\theta})$ is a sufficiently accurate approximation of $\nabla \widehat{\mathfrak{J}}(\boldsymbol{\theta})$ (i.e. securing descent properties with respect to $\widehat{\mathfrak{J}}$ at $\boldsymbol{\theta}$) we use the discrete gradient, e.g., in the Adam optimizer [40], to minimize $\widehat{\mathfrak{J}}_D^{M,h}(\boldsymbol{\theta})$. Next we summarize our overall computational procedure in Algorithm 3.1. Upon successful termination it produces neural network parameters and other outputs by setting $\hat{it} := it + 1$. In Algorithm 3.1, $\text{grad}_\boldsymbol{\theta}$ refers to automatic differentiation with respect to the NN parameters. The typical optimizer of choice also depends on hyperparameters. For the Adam optimizer, these include selecting a learning rate $lr \in \mathbb{R}_+$ or a schedule of learning rates $lr : \mathbb{N} \rightarrow \mathbb{R}_+$ with $it \mapsto lr(it)$, as well as specifying values for $\beta_1^{Ad} \in \mathbb{R}_+$ and $\beta_2^{Ad} \in \mathbb{R}_+$ for the moving average update, and setting a batch size. We initialize $\boldsymbol{\theta}^{(0)}$ using the Glorot scheme [24], but $\boldsymbol{\theta}^{(0)}$ can also be obtained by solving a neighboring, yet simpler problem [26, 70]. For an overview of standard NN optimization techniques, we refer exemplarily to [25] and the references therein.

4. An application in heat conduction. In this section, we focus on the example of heat conduction with respect to both, the coarse and the fine scale, respectively. For this purpose let $u_{\boldsymbol{\theta},n}$ denote the *parameterization* of $\mathcal{L}[u_{\boldsymbol{\theta},n}]$. Specifically, we study our hybrid approach in view of its embedded upscaling process.

Algorithm 3.1 Hybrid physics-informed NN training

Input: Tolerance tol , max. number of iterations it_{\max} , initial NN parameters $\boldsymbol{\theta}^{(0)}$, initial state FEM coefficients $\mathbf{y}_h(\boldsymbol{\theta}^{(0)})$, optimizer hyperparameters.

Output: NN parameters $\hat{\boldsymbol{\theta}} := \boldsymbol{\theta}^{(it)}$, control variable $v_{\hat{\boldsymbol{\theta}},n}^M \approx u_{\hat{\boldsymbol{\theta}},n}^{\varepsilon,M}$, state variable $\mathbf{y}_h(\hat{\boldsymbol{\theta}}) \in \mathbb{R}^{N_h}$.

- 1: **while** $0 \leq it \leq it_{\max} - 1$ or $\widehat{\mathcal{J}}^M(v_{\boldsymbol{\theta}^{(it)},n}^M) > tol$ **do**
- 2: Solve the adjoint system $\mathbb{B}_h^{\text{ad}}[\boldsymbol{\theta}^{(it)}] \mathbf{p}_h = 2\tau_2(\mathbb{P}_h[\boldsymbol{\theta}^{(it)}] - \mathbb{P}_h[\mathbf{y}_h(\boldsymbol{\theta}^{(it)})])$
- 3: Compute $\nabla_{\boldsymbol{\theta}} \widehat{\mathcal{J}}_D^{M,h}(\mathbf{y}_h(\boldsymbol{\theta}^{(it)}), \boldsymbol{\theta}^{(it)}) := \text{grad}_{\boldsymbol{\theta}}(\widehat{\mathcal{J}}_D^{M,h}(\boldsymbol{\theta}^{(it)}))$
- 4: Assemble the total gradient $\nabla \widehat{\mathcal{J}}_D^{M,h}(\boldsymbol{\theta}^{(it)})$
- 5: Update weights $\boldsymbol{\theta}^{(it+1)} \leftarrow \text{Optimizer}(\nabla \widehat{\mathcal{J}}_D^{M,h}(\boldsymbol{\theta}^{(it)}), \text{optimizer hyperparameters})$
- 6: Solve the state system $\mathbb{B}_h[\boldsymbol{\theta}^{(it+1)}] \mathbf{y}_h(\boldsymbol{\theta}^{(it+1)}) = \mathbb{F}_h$
- 7: $it \leftarrow it + 1$
- 8: **end while**

4.1. Upscaling-based parameterization. Our exemplary stationary heat transfer problem in $\bar{\Omega} = [0, 1]^2$ is defined as follows:

$$(4.1) \quad -\nabla \cdot (\mathbf{K}^\varepsilon \nabla w^\varepsilon) = q, \quad \text{in } \Omega, \quad \text{and } w^\varepsilon = 0, \quad \text{on } \partial\Omega,$$

where w^ε is the temperature field, $q \in L^2(\Omega)$ is the source term, $\mathbf{K}^\varepsilon \in C^{0,1}(\bar{\Omega}, \mathbb{R}_+)$ is a Lipschitz continuous coefficient, and $\varepsilon \in \mathbb{R}_+$ is a small parameter indicating the fine scale length. In addition, it holds that

$$(4.2) \quad \exists \alpha, \beta \in \mathbb{R}_+ : \alpha \leq \mathbf{K}^\varepsilon(x) \leq \beta, \quad \forall x \in \bar{\Omega},$$

We assume further that $\|\nabla \mathbf{K}^\varepsilon\|_{L^\infty(\Omega)} \leq \frac{c_{\mathbf{K}}}{\varepsilon}$, where $c_{\mathbf{K}} \in \mathbb{R}_+$ is ε -independent.

Solving (4.1) using finite elements can be computationally demanding due to the requirement $h \ll \varepsilon$ for a mesh size $h \in \mathbb{R}_+$ and $\varepsilon \ll 1$ in order to resolve the fine scale behaviour numerically. We aim to efficiently characterize material properties of Ω and determine a computationally feasible coarse-scale (homogenized) counterpart of (4.1). In this vein, the concept of G -convergence is employed to formalize the notion of a homogenized equation and the related effective material; see, e.g., [37].

DEFINITION 4.1. A coefficient sequence $\{\mathbf{K}^\varepsilon(\cdot)\}$ is said to G -converge to $\mathbf{K}^*(\cdot)$ as $\varepsilon \rightarrow 0$, if for any $q \in H^{-1}(\Omega)$ the sequence of solutions $\{w^\varepsilon\}$ of (4.1) satisfies

$$(4.3) \quad w^\varepsilon \rightharpoonup w^0 \quad \text{in } H_0^1(\Omega), \quad \mathbf{K}^\varepsilon \nabla w^\varepsilon \rightharpoonup \mathbf{K}^* \nabla w^0 \quad \text{in } L^2(\Omega),$$

where w^0 is the solution to the homogenized equation

$$-\nabla \cdot (\mathbf{K}^* \nabla w^0) = q, \quad \text{in } \Omega, \quad \text{and } w^0 = 0, \quad \text{on } \partial\Omega.$$

Various techniques exist to find the G -limit. Their respective applicability, however, depends on the specific problem and properties of the underlying medium. If such a G -limit exists, then it does not depend on q and on the boundary data on $\partial\Omega$. We also note that the existence of \mathbf{K}^* for general heterogeneous media still remains an open problem. Often, the representative volume element (RVE) technique can be applied to find an approximation of \mathbf{K}^* . This approach is widely utilized in engineering

applications; see, e.g., [14, 20, 22, 23]. Here we state its equivalent characterization via weak convergence of gradients and fluxes in (4.3): For any measurable set $\mathcal{V} \subseteq \Omega$ of measure $|\mathcal{V}| > 0$ and $\langle \cdot \rangle_{\mathcal{V}} = \frac{1}{|\mathcal{V}|} \int_{\mathcal{V}} \cdot \, dx$ (understood component-wise), one has

$$(4.4) \quad \lim_{\varepsilon \rightarrow 0} \langle \nabla w^\varepsilon \rangle_{\mathcal{V}} = \langle \nabla w^0 \rangle_{\mathcal{V}}, \quad \lim_{\varepsilon \rightarrow 0} \langle \mathbf{K}^\varepsilon \nabla w^\varepsilon \rangle_{\mathcal{V}} = \langle \mathbf{K}^* \nabla w^0 \rangle_{\mathcal{V}}.$$

The existence of the above limits for general heterogeneous media is difficult to verify. Thus, here we only assume that these limits exist; see also Assumption 2.6. Further, we introduce the following approximations:

$$\langle \nabla w^\varepsilon \rangle_{\mathcal{V}} \approx \lim_{\varepsilon \rightarrow 0} \langle \nabla w^\varepsilon \rangle_{\mathcal{V}} = \langle \nabla w^0 \rangle_{\mathcal{V}}, \quad \langle \mathbf{K}^\varepsilon \nabla w^\varepsilon \rangle_{\mathcal{V}} \approx \lim_{\varepsilon \rightarrow 0} \langle \mathbf{K}^\varepsilon \nabla w^\varepsilon \rangle_{\mathcal{V}} \approx \widetilde{\mathbf{K}} \langle \nabla w^0 \rangle_{\mathcal{V}},$$

where $\widetilde{\mathbf{K}}$ is defined as follows.

DEFINITION 4.2 (**Upscaled coefficient**). *The upscaled coefficient $\widetilde{\mathbf{K}}$ satisfies*

$$(4.5) \quad \langle \mathbf{K}^\varepsilon \nabla w^\varepsilon \rangle_{\mathcal{V}} = \widetilde{\mathbf{K}}(x) \langle \nabla w^\varepsilon \rangle_{\mathcal{V}}, \quad \text{for all } x \in \mathcal{V},$$

where $\widetilde{\mathbf{K}}$ is a 2×2 tensor on \mathcal{V} approximating \mathbf{K}^* on \mathcal{V} .

Note that $\widetilde{\mathbf{K}}$ is constant on \mathcal{V} as a consequence of its definition. Besides, it is beneficial to consider $\widetilde{\mathbf{K}}$ as a tensor for anisotropic materials. Further we observe that in our concrete setting, two solutions of the fine-scale problem are required to obtain $\widetilde{\mathbf{K}}$ from (4.5). In contrast to \mathbf{K}^* , boundary conditions may then affect $\widetilde{\mathbf{K}}$. Of course, it is very desirable to identify a set of boundary conditions such that the dependence of $\widetilde{\mathbf{K}}$ on them is weak. In our application context, we choose the linear temperature drop boundary conditions $w_i^\varepsilon = x_i$ on $\partial\Omega$, $i = 1, 2$, but periodic boundary conditions or temperature drop no-flow conditions can be applied as well. Their related analyses are similar; compare [20, 46, 68]. The calculation of the upscaled thermal conductivity coefficient then leads to the following fine-scale problems: For $i \in \{1, 2\}$, find $w_i^\varepsilon : \Omega \rightarrow \mathbb{R}$ with

$$(4.6) \quad -\nabla \cdot (\mathbf{K}^\varepsilon \nabla w_i^\varepsilon) = q, \quad \text{in } \Omega, \quad \text{and} \quad w_i^\varepsilon = x_i, \quad \text{on } \partial\Omega.$$

We note that $q = 0$ is typically chosen to prevent any influence of the source term on $\widetilde{\mathbf{K}}$. However, our multiscale solver is designed for computations of fine-scale solutions with $q \neq 0$, and setting $q = 0$ defines a special case for our NN-based homogenization scheme below. Therefore, a more general form of (4.6) is considered, but the influence of q on $\widetilde{\mathbf{K}}$ is assumed to be rather weak. The upscaling process is described in Algorithm 4.1; cf. [68, Section 4].

Clearly, we need to ensure that the matrix of averaged gradients in (4.7) is invertible. This requires the partition $\{\mathcal{V}_j\}$ to be sufficiently heterogeneous with each \mathcal{V}_j of “reasonable” size to prevent linear dependence between $\widetilde{\mathbf{T}}_1^j$ and $\widetilde{\mathbf{T}}_2^j$. Algorithm 4.1 is based on problem-dependent constitutive relations. In our case, we apply Fourier’s law of heat conduction (4.7); cf. [22, 46]. In view of other applications, Darcy’s law is used for porous media flows [27, 33, 68] as the relation between fluid velocity and pressure, and Hooke’s law is applied [12] in elasticity to relate stress and strain fields.

For $\mathcal{V} = \Omega = (0, 1)^2$, we derive a simplified formula for the upscaled coefficient; cf. [68]. For this purpose, it is convenient to study problem (4.6) as a problem with homogeneous Dirichlet boundary conditions. Let $u^{x_i} := x_i$ be the extension of our boundary conditions to Ω and consider the problem

$$(4.8) \quad -\nabla \cdot (\mathbf{K}^\varepsilon \nabla u_i^\varepsilon) = q + \nabla \cdot (\mathbf{K}^\varepsilon \nabla u^{x_i}), \quad \text{in } \Omega, \quad \text{and} \quad u_i^\varepsilon = 0, \quad \text{on } \partial\Omega.$$

Algorithm 4.1 Upscaling algorithm

Input: $\Omega = \bigcup_{j=1}^N \mathcal{V}_j$ with $\mathcal{V}_i \cap \mathcal{V}_j = \emptyset$, $i \neq j$, the solutions $\mathbf{w}^\varepsilon = \{w_1^\varepsilon, w_2^\varepsilon\}$ of (4.6).

Output: The upcaled coefficient $\widetilde{\mathbf{K}}$.

- 1: **for** $j \in \{1, \dots, N\}$ **do**
- 2: Compute $\widetilde{\mathbf{F}}_i^j := \langle \mathbf{K}^\varepsilon \nabla w_i^\varepsilon \rangle_{\mathcal{V}_j} \in \mathbb{R}^2$, $\widetilde{\mathbf{T}}_i^j := \langle \nabla w_i^\varepsilon \rangle_{\mathcal{V}_j} \in \mathbb{R}^2$ for $i \in \{1, 2\}$.
- 3: Insert $\widetilde{\mathbf{F}}_i^j$ and $\widetilde{\mathbf{T}}_i^j$ into (4.5) and find $\widetilde{\mathbf{K}}^j \in \mathbb{R}^{2 \times 2}$ from the matrix equation:

$$(4.7) \quad \begin{pmatrix} \widetilde{\mathbf{K}}_{11}^j & \widetilde{\mathbf{K}}_{12}^j \\ \widetilde{\mathbf{K}}_{21}^j & \widetilde{\mathbf{K}}_{22}^j \end{pmatrix} \begin{pmatrix} (\widetilde{\mathbf{T}}_1^j)_1 & (\widetilde{\mathbf{T}}_2^j)_1 \\ (\widetilde{\mathbf{T}}_1^j)_2 & (\widetilde{\mathbf{T}}_2^j)_2 \end{pmatrix} = \begin{pmatrix} (\widetilde{\mathbf{F}}_1^j)_1 & (\widetilde{\mathbf{F}}_2^j)_1 \\ (\widetilde{\mathbf{F}}_1^j)_2 & (\widetilde{\mathbf{F}}_2^j)_2 \end{pmatrix}.$$

4: **end for**

5: Get $\widetilde{\mathbf{K}}$ with $\widetilde{\mathbf{K}}(x) = \widetilde{\mathbf{K}}^j$ for $x \in \mathcal{V}_j$

Now, we apply Algorithm 4.1 to $\widetilde{\mathbf{F}}_i := \langle \mathbf{K}^\varepsilon \nabla w_i^\varepsilon \rangle_\Omega$ and $\widetilde{\mathbf{T}}_i := \langle \nabla w_i^\varepsilon \rangle_\Omega$. Since $w_i^\varepsilon = u_i^\varepsilon + u^{x_i}$ and $\nabla u^{x_i} = \mathbf{e}_i$, where $\mathbf{e}_i \in \mathbb{R}^2$ denotes the i -th unit vector, the divergence theorem yields

$$(4.9) \quad \langle \nabla w_i^\varepsilon \rangle_\Omega = \int_{\partial\Omega} u_i^\varepsilon \boldsymbol{\eta} \, ds + \int_\Omega \mathbf{e}_i \, dx = \mathbf{e}_i,$$

where $\boldsymbol{\eta}(x)$ is the outward unit normal at $x \in \partial\Omega$. Inserting (4.9) into (4.7), we get

$$(4.10) \quad \widetilde{\mathbf{K}}_{ij} = \int_\Omega \mathbf{K}^\varepsilon \partial_{x_j} w_i^\varepsilon \, dx = \int_\Omega \mathbf{K}^\varepsilon (\partial_{x_j} u_i^\varepsilon + \delta_{ij}) \, dx,$$

where δ_{ij} denotes the Kronecker delta symbol and $\partial_{x_j} := \frac{\partial}{\partial x_j}$.

4.2. Analysis of the model equations. From now on we assume that the following assumption is satisfied.

ASSUMPTION 4.3. *Assume that $u^\varepsilon := u_1^\varepsilon$ is the solution to problem (4.8). Moreover, $\widetilde{\mathbf{K}}[u^\varepsilon] := \widetilde{\mathbf{K}} \in \mathbb{R}^{2 \times 2}$, where $\widetilde{\mathbf{K}}_{12} = \widetilde{\mathbf{K}}_{21} \geq 0$ and $\widetilde{\mathbf{K}}_{22} \geq 0$ are provided to us and fixed, and $\widetilde{\mathbf{K}}[u^\varepsilon]_{11} = \int_\Omega \mathbf{K}^\varepsilon (\partial_{x_1} u^\varepsilon + 1) \, dx$ is according to (4.10).*

Assumption 4.3 implies that one needs to solve the model fine-scale problem (4.8) only for $i = 1$ to get $\widetilde{\mathbf{K}}_{11}$. We note that for periodic coefficients \mathbf{K}^ε with period ε , $\widetilde{\mathbf{K}}_{12} = \widetilde{\mathbf{K}}_{21} = 0$ and $\widetilde{\mathbf{K}}[u^\varepsilon] = \widetilde{\mathbf{K}}[u^\varepsilon]_{11} I$, where $I \in \mathbb{R}^{2 \times 2}$ is the identity.

Next, we show that the assumptions of Section 2 are satisfied by our fine- and coarse-scale model problems. For this purpose, let $X := C^k(\bar{\Omega})$ for some $k \geq 2$, $U := H^2(\Omega)$, $U_0 := H^2(\Omega) \cap H_0^1(\Omega)$ and $V := H^{1/2}(\Omega)$ be equipped with the norms

$$\begin{aligned} \|v\|_X &= \sum_{|\mathbf{a}| \leq 2} \sup_{x \in \Omega} |\partial_x^\mathbf{a} v(x)|, & \|v\|_U &= \|v\|_{U_0} = \left(\sum_{|\mathbf{a}| \leq 2} \|\partial_x^\mathbf{a} v\|_{L^2(\Omega)}^2 \right)^{1/2}, \\ \|v\|_V &= \left(\|v\|_{L^2(\Omega)}^2 + \int_\Omega \int_\Omega \frac{|v(x) - v(y)|^2}{|x - y|^{d+1}} \, dx dy \right)^{1/2}, \end{aligned}$$

respectively. Recall that X is dense in U and $\|u\|_U \leq |\Omega|^{1/2} \|u\|_X$ for $v \in X$, i.e. $X \hookrightarrow U$. Let $H := L^2(\Omega)$, $Z := L^2(\partial\Omega)$, $Y := H_0^1(\Omega)$, $Y^* = H^{-1}(\Omega)$ with $Y \hookrightarrow H \hookrightarrow Y^*$, where Y is compactly embedded into H by the Rellich–Kondrachov Theorem. We

define the following linear operators

$$\mathcal{A}^\varepsilon : U \rightarrow H, \quad v \mapsto \mathcal{A}^\varepsilon v = -\nabla \cdot (\mathbf{K}^\varepsilon \nabla v), \quad \text{and } \mathcal{B} : U \rightarrow Z, \quad v \mapsto \mathcal{B}v = v|_{\partial\Omega}.$$

We cast our model fine-scale problem into the operator form

$$(4.11) \quad \mathcal{A}^\varepsilon u = f^\varepsilon, \quad \text{in } H, \quad \text{and } \mathcal{B}u = 0, \quad \text{in } Z,$$

with $f^\varepsilon := q - \mathcal{A}^\varepsilon u^{x_1} \in L^2(\Omega) = H$. By the Lax–Milgram lemma, (4.11) has a unique solution $u^\varepsilon \in Y$, and we have $w_1^\varepsilon = u^\varepsilon + u^{x_1}$. The next proposition shows that $u^\varepsilon \in U$, thereby confirming Assumption 2.1, and that Assumption 2.3 is satisfied.

PROPOSITION 4.4. *There exist $C_s^\varepsilon \in \mathbb{R}_+$ and $C_b^\varepsilon \in \mathbb{R}_+$ such that*

$$(4.12) \quad C_s^\varepsilon \|u\|_U^2 \leq \|\mathcal{A}^\varepsilon u\|_H^2 \leq C_b^\varepsilon \|u\|_U^2, \quad \forall u \in U_0,$$

where $C_s^\varepsilon \rightarrow 0$, $C_b^\varepsilon \rightarrow \infty$ as $\varepsilon \rightarrow 0$.

Proof. We multiply (4.11) (with $u = u^\varepsilon$) by u^ε and integrate by parts to get

$$\alpha \int_\Omega |\nabla u^\varepsilon|^2 \, dx \leq \int_\Omega \mathbf{K}^\varepsilon \nabla u^\varepsilon \cdot \nabla u^\varepsilon \, dx = \int_\Omega q u^\varepsilon - \mathbf{K}^\varepsilon \partial_{x_1} u^\varepsilon \, dx.$$

Using the Cauchy–Schwarz and Poincaré inequalities, we get

$$(4.13) \quad \|\nabla u^\varepsilon\|_H \leq \frac{\beta + c_p \|q\|_H}{\alpha},$$

where the Poincaré constant $c_p \in \mathbb{R}_+$ depends only on Ω , and β is according to (4.2). Note that problem (4.11) can be written as follows:

$$-\Delta u^\varepsilon = g^\varepsilon := \frac{f^\varepsilon + \nabla \mathbf{K}^\varepsilon \cdot \nabla u^\varepsilon}{\mathbf{K}^\varepsilon}, \quad \text{in } \Omega, \quad \text{and } u^\varepsilon = 0, \quad \text{on } \partial\Omega.$$

Invoking a standard $H^2(\Omega)$ regularity result for convex domains [28], we get

$$(4.14) \quad \|u^\varepsilon\|_U \leq \widehat{C} \|g^\varepsilon\|_H \leq \frac{\widehat{C}}{\alpha} (\|q\|_H + (\|\nabla u^\varepsilon\|_H + 1) \|\nabla \mathbf{K}^\varepsilon\|_{L^\infty(\Omega)}).$$

where $\widehat{C} = \widehat{C}(\Omega) \in \mathbb{R}_+$. Using (4.13) and $\|\nabla \mathbf{K}^\varepsilon\|_{L^\infty(\Omega)} \leq \frac{c_{\mathbf{K}}}{\varepsilon}$, we obtain the estimate

$$(4.15) \quad \|u^\varepsilon\|_U \leq \frac{\widehat{C}}{\alpha} \left(\left(1 + \frac{\beta}{\alpha}\right) \frac{c_{\mathbf{K}}}{\varepsilon} + \left(1 + \frac{c_{\mathbf{K}} c_p}{\varepsilon \alpha}\right) \|q\|_H \right).$$

The bound (4.15) implies that $\|(\mathcal{A}^\varepsilon)^{-1}\| \leq (C_1 + \frac{C_2}{\varepsilon}) < \infty$ for $\varepsilon > 0$ and some ε -independent $C_1, C_2 \in \mathbb{R}_+$, from where the lower bound in (4.12) readily follows. Using the Young and the Cauchy–Schwarz inequalities, for $u \in U$, we get

$$(4.16) \quad \|\mathcal{A}^\varepsilon u\|_H^2 \leq 2(\|\nabla \mathbf{K}^\varepsilon \cdot \nabla u\|_H^2 + \|\mathbf{K}^\varepsilon \Delta u\|_H^2) \leq \left(\frac{C}{\varepsilon^2} + \beta^2 \right) \|u\|_U^2,$$

where $C \in \mathbb{R}_+$ is ε -independent. This proves the upper bound in (4.12). \square

The estimate (4.12) and interpolation techniques are used to verify the lower bound in Assumption 2.3 including $\|\mathcal{B}u\|_Z$, see [73, Lemma 4.1] and references therein. The upper bound in Assumption 2.3 follows from (4.16) and the trace inequality. These estimates are summarized in the following proposition.

PROPOSITION 4.5. *There exist $\bar{C}_s^\varepsilon \in \mathbb{R}_+$ and $C_b^\varepsilon \in \mathbb{R}_+$ such that*

$$(4.17) \quad \bar{C}_s^\varepsilon \|u\|_V^2 \leq \|\mathcal{A}^\varepsilon u\|_H^2 + \|\mathcal{B}u\|_Z^2 \leq C_b^\varepsilon \|u\|_U^2, \quad \forall u \in U,$$

where $\bar{C}_s^\varepsilon \rightarrow 0$, $C_b^\varepsilon \rightarrow \infty$ as $\varepsilon \rightarrow 0$.

The next result [69, Theorem 3.3] shows that NNs with smooth activation functions are universal approximators of $C^k(\bar{\Omega})$, verifying Assumption 2.5 for $X := C^2(\bar{\Omega})$.

PROPOSITION 4.6. *Suppose that $\sigma \in C^\infty(\mathbb{R})$, $\sigma^{(s)}(0) \neq 0$ for $s = 0, 1, \dots$, and $\bar{\Omega} := [0, 1]^d$. If $v \in C^k(\bar{\Omega})$, then there exists an architecture $\bar{\mathbf{n}}$ with one hidden layer and $v_{\theta, n} \in \mathfrak{N}_{\theta, n}$ such that*

$$\sup_{x \in \bar{\Omega}} |\partial_x^{\mathbf{a}} v(x) - \partial_x^{\mathbf{a}} v_{\theta, n}(x)| = \mathcal{O}\left(\frac{1}{n^{(k-|\mathbf{a}|)/d}} \omega\left(\partial_x^{\mathbf{b}} v, \frac{1}{n^{1/2}}\right)\right)$$

holds for all multi-indices \mathbf{a}, \mathbf{b} with $|\mathbf{a}| \leq k$, $|\mathbf{b}| = k$, where, for $\delta_c > 0$, $\omega(v, \delta_c) = \sup\{|v(x) - v(y)| : |x - y| \leq \delta_c, x, y \in \bar{\Omega}\}$ is the modulus of continuity of v .

For example, the swish function $\sigma(x) = x \text{sigmoid}(x)$ satisfies the prerequisites of Proposition 4.6, but the widely-used $\tanh(x)$ does not satisfy $\sigma^{(2)}(0) \neq 0$ rendering Proposition 4.6 non-applicable. The following result [17, Theorem 5.1] is then useful.

PROPOSITION 4.7. *Suppose that $\sigma(x) = \tanh(x)$ and $\bar{\Omega} := [0, 1]^d$. If $v \in C^k(\bar{\Omega})$, then there exists an architecture $\bar{\mathbf{n}}$ with two hidden layers and $v_{\theta, n} \in \mathfrak{N}_{\theta, n}$ such that $\|v - v_{\theta, n}\|_{W^{m, \infty}(\bar{\Omega})} = \mathcal{O}(n^{-(k-m)})$ holds¹, where $\|w\|_{W^{m, \infty}(\bar{\Omega})} = \max_{|\mathbf{a}| \leq m} \sup_{x \in \bar{\Omega}} |\partial_x^{\mathbf{a}} w(x)|$.*

From the prerequisites of Proposition 4.7 we infer $X := C^k(\bar{\Omega})$ with $k > 2$ as $m = 2$ in our example. Clearly, $\mathfrak{N}_{\theta, n} \subset X$ and $\|v\|_X \leq C\|v\|_{W^{2, \infty}(\bar{\Omega})}$ for $v \in X$ and some $C \in \mathbb{R}_+$. The latter implies $X \subset \overline{\cup_n \mathfrak{N}_{\theta, n}}$, thereby verifying Assumption 2.5 for the hyperbolic tangent activation function.

Our model coarse-scale problem in its weak form reads: Find $y(u^\varepsilon) \in Y$ such that

$$(4.18) \quad b_{\mathcal{L}}[u^\varepsilon](y(u^\varepsilon), v) = \langle \tilde{f}, v \rangle_{Y^*, Y} \quad \forall v \in Y,$$

where $\tilde{f} := q + \nabla \cdot (\widetilde{\mathbf{K}}[u^\varepsilon] \nabla u^{x_1})$ and the forms are defined as follows:

$$b_{\mathcal{L}}[u^\varepsilon](w, v) := \int_{\Omega} \widetilde{\mathbf{K}}[u^\varepsilon] \nabla w \cdot \nabla v \, dx, \quad \langle \tilde{f}, v \rangle_{Y^*, Y} = \int_{\Omega} qv \, dx - \int_{\Omega} \widetilde{\mathbf{K}}[u^\varepsilon] e_1 \cdot \nabla v \, dx.$$

Since $\widetilde{\mathbf{K}}[u^\varepsilon]$ is a constant matrix, $\int_{\Omega} \partial_{x_j} v \, dx = 0$ for $j \in \{1, 2\}$ and $v \in Y$, it holds:

$$\int_{\Omega} \widetilde{\mathbf{K}}[u^\varepsilon] e_1 \cdot \nabla v \, dx = \sum_{j=1}^2 (\widetilde{\mathbf{K}}[u^\varepsilon])_{j1} \int_{\Omega} \partial_{x_j} v \, dx = 0.$$

To study the fine-to-coarse scale mapping, we need the following related map:

$$(4.19) \quad u \in U \mapsto \widetilde{\mathbf{K}}[u] \in \mathbb{R}^{2 \times 2}, \quad u \mapsto \begin{pmatrix} \widetilde{\mathbf{K}}[u]_{11} & \widetilde{\mathbf{K}}[u]_{12} \\ \widetilde{\mathbf{K}}[u]_{21} & \widetilde{\mathbf{K}}[u]_{22} \end{pmatrix},$$

where $\widetilde{\mathbf{K}}[u]_{11} = \int_{\Omega} \mathbf{K}^\varepsilon(\partial_{x_1} u + 1) \, dx$. Firstly, we prove the following.

¹We state the asymptotic convergence rate, but explicit constants are estimated in [17].

LEMMA 4.8. *The mapping $u \in U \mapsto \widetilde{\mathbf{K}}[u] \in \mathbb{R}^{2 \times 2}$ defined by (4.19) is Lipschitz continuous, i.e., for $u_1, u_2 \in U$ we have*

$$(4.20) \quad \|\widetilde{\mathbf{K}}[u_1] - \widetilde{\mathbf{K}}[u_2]\| \leq |\Omega|^{1/2} \beta \|u_1 - u_2\|_U,$$

$$(4.21) \quad \|\widetilde{\mathbf{K}}[u_1] - \widetilde{\mathbf{K}}[u_2]\| \leq |\Omega|^{1/2} \varepsilon^{-1} c_{\mathbf{K}} \|u_1 - u_2\|_V,$$

with $\beta > 0$ from (4.2), and the Frobenius norm $\|\widetilde{\mathbf{K}}[u]\| := \left(\sum_{i,j=1}^2 (\widetilde{\mathbf{K}}[u]_{ij})^2 \right)^{\frac{1}{2}}$ of $\widetilde{\mathbf{K}}[u]$.

Proof. The Cauchy–Schwarz inequality and (4.2) yield

$$(4.22) \quad |(\widetilde{\mathbf{K}}[u_1])_{11} - (\widetilde{\mathbf{K}}[u_2])_{11}| \leq |\Omega|^{1/2} \beta \|\partial_{x_1} u_1 - \partial_{x_1} u_2\|_H \leq |\Omega|^{1/2} \beta \|u_1 - u_2\|_U.$$

In our case, $\widetilde{\mathbf{K}}_{12}$, $\widetilde{\mathbf{K}}_{21}$, $\widetilde{\mathbf{K}}_{22}$ are fixed, hence we get $\|\widetilde{\mathbf{K}}[u_1] - \widetilde{\mathbf{K}}[u_2]\| = |(\widetilde{\mathbf{K}}[u_1])_{11} - (\widetilde{\mathbf{K}}[u_2])_{11}|$ and (4.20) follows.

Next, we write $\widetilde{\mathbf{K}}[u]_{11} = \int_{\Omega} \mathbf{K}^\varepsilon - (\partial_{x_1} \mathbf{K}^\varepsilon) u \, dx$. The Cauchy–Schwarz inequality, $\|\nabla \mathbf{K}^\varepsilon\|_{L^\infty(\Omega)} \leq \frac{c_{\mathbf{K}}}{\varepsilon}$ and the continuous embedding $V \hookrightarrow H$ imply that

$$\|\widetilde{\mathbf{K}}[u_1] - \widetilde{\mathbf{K}}[u_2]\| \leq \int_{\Omega} |\partial_{x_1} \mathbf{K}^\varepsilon (u_2 - u_1)| \, dx \leq |\Omega|^{1/2} \varepsilon^{-1} c_{\mathbf{K}} \|u_1 - u_2\|_V. \quad \square$$

We note that (4.21) readily implies (3.19). Next, we show that Assumption 2.4 holds, assuming that the influence of q is rather weak.

PROPOSITION 4.9. *Suppose that $\|q\|_H \leq \frac{\alpha(\nu + \|\nabla u^\varepsilon\|_H^2)}{\|u^\varepsilon\|_H}$ for some $0 < \nu < 1$ and $\alpha \in \mathbb{R}_+$ from (4.2). Then, there exists $B_{\bar{r}}(u^\varepsilon) = \{v : \|u^\varepsilon - v\|_U \leq \bar{r}\} \subset U$ and $C_b, C_c \in \mathbb{R}_+$ such that (2.5) holds for all $v, w \in Y$ and $u \in B_{\bar{r}}(u^\varepsilon)$.*

Proof. Set $\mathbf{v}^\varepsilon = (u^\varepsilon, 0)$. Then $\nabla \cdot \mathbf{v}^\varepsilon = \partial_{x_1} u^\varepsilon$ and the divergence theorem yield

$$(4.23) \quad \int_{\Omega} \partial_{x_1} u^\varepsilon \, dx = \int_{\Omega} \nabla \cdot \mathbf{v}^\varepsilon \, dx = \int_{\partial\Omega} \mathbf{v}^\varepsilon \cdot \boldsymbol{\eta} \, dx = 0,$$

since $u^\varepsilon|_{\partial\Omega} = 0$. From (4.10), we deduce

$$(4.24) \quad \widetilde{\mathbf{K}}[u^\varepsilon]_{11} = \mathbf{e}_1 \cdot \widetilde{\mathbf{K}}[u^\varepsilon] \mathbf{e}_1 = \langle \nabla w_1^\varepsilon \cdot \mathbf{K}^\varepsilon \nabla w_1^\varepsilon \rangle_{\Omega} - \langle \nabla u^\varepsilon \cdot \mathbf{K}^\varepsilon \nabla w_1^\varepsilon \rangle_{\Omega}.$$

Integrating the last term in (4.24) by parts gives

$$(4.25) \quad \int_{\Omega} \nabla u^\varepsilon \cdot \mathbf{K}^\varepsilon \nabla w_1^\varepsilon \, dx = \int_{\partial\Omega} u^\varepsilon (\mathbf{K}^\varepsilon \nabla w_1^\varepsilon \cdot \boldsymbol{\eta}) \, ds - \int_{\Omega} \nabla \cdot (\mathbf{K}^\varepsilon \nabla w_1^\varepsilon) u^\varepsilon \, dx,$$

where $u^\varepsilon|_{\partial\Omega} = 0$ and $-\nabla \cdot (\mathbf{K}^\varepsilon \nabla w_1^\varepsilon) = q$ in Ω . Therefore, from (4.23) we obtain

$$\begin{aligned} \widetilde{\mathbf{K}}[u^\varepsilon]_{11} &= \langle \nabla w_1^\varepsilon \cdot \mathbf{K}^\varepsilon \nabla w_1^\varepsilon \rangle_{\Omega} - \int_{\Omega} q u^\varepsilon \, dx \geq \alpha \int_{\Omega} |\nabla w_1^\varepsilon|^2 \, dx - \int_{\Omega} q u^\varepsilon \, dx \\ &= \alpha \int_{\Omega} (|\nabla u^\varepsilon|^2 + 2\partial_{x_1} u^\varepsilon + 1) \, dx - \int_{\Omega} q u^\varepsilon \, dx \geq \alpha(1 + \|\nabla u^\varepsilon\|_H^2) - \int_{\Omega} q u^\varepsilon \, dx. \end{aligned}$$

The Cauchy–Schwarz inequality and our (amplitude) assumption on q give us

$$\widetilde{\mathbf{K}}[u^\varepsilon]_{11} \geq \alpha(1 + \|\nabla u^\varepsilon\|_H^2) - \|q\|_H \|u^\varepsilon\|_H \geq (1 - \nu)\alpha =: C_\alpha.$$

Integration by parts, using the equation satisfied by u^ε , the Cauchy–Schwarz inequality, and (4.13) result in the estimate

$$|\widetilde{\mathbf{K}}[u^\varepsilon]_{11}| \leq \beta + \beta \|\nabla u^\varepsilon\|_H \leq \beta + \beta \left(\frac{\beta + c_p \|q\|_H}{\alpha} \right) =: C_\beta.$$

Let $0 \leq \bar{s} \leq \nu(1 - \nu)\alpha$ and $\bar{r} = \frac{\bar{s}}{|\Omega|^{1/2}\beta}$. Then (4.20) implies that for $u \in B_{\bar{r}}(u^\varepsilon)$ it holds:

$$(4.26) \quad 0 < (1 - \nu)C_\alpha \leq \widetilde{\mathbf{K}}[u^\varepsilon]_{ii} - \bar{r} \leq \widetilde{\mathbf{K}}[u]_{11} \leq \widetilde{\mathbf{K}}[u^\varepsilon]_{11} + \bar{r} \leq C_\beta + \nu(1 - \nu)\alpha.$$

Then, we set $C_c := (1 - \nu)C_\alpha$ and $C_b := C_\beta + \nu(1 - \nu)\alpha$ and apply the standard coercivity and continuity estimates to complete the proof. \square

The Lax–Milgram lemma and Proposition 4.9 imply that for $u \in B_{\bar{r}}(u^\varepsilon)$ there exist a unique solution $y(u) \in Y$ of (4.18) with $\|y(u)\|_Y \leq C\|q\|_H$, where $C \in \mathbb{R}_+$ is independent of u , but also of ε , since \bar{r} , C_c and C_b are independent of ε in Proposition 4.9. The constant coefficient in (4.18) implies that $y(u) \in U$ for all $u \in B_{\bar{r}}(u^\varepsilon)$, hence we use (2.10). Proposition 4.9 motivates the following rather general assumption.

ASSUMPTION 4.10. *For $q \in H$, $\mathbf{K}^\varepsilon \in C^{0,1}(\bar{\Omega})$, one can find $\bar{r}^\varepsilon \in \mathbb{R}_+$ and respective $B_{\bar{r}^\varepsilon}(u^\varepsilon) \subset U$ such that $y(u) \in Y$ exists and $\|y(u)\|_Y \leq C\|q\|_H$ for all $u \in B_{\bar{r}^\varepsilon}(u^\varepsilon)$, where $C \in \mathbb{R}_+$ is independent of u .*

Next, we verify Assumption 3.1 about the continuity of our fine-to-coarse scale map.

PROPOSITION 4.11. *Suppose that Assumption 4.10 holds and $\{u_k^\varepsilon\} \subset B_{\bar{r}^\varepsilon}(u^\varepsilon) \cap X$ is an approximating sequence of u_ε . Then $S(u_k^\varepsilon) \rightharpoonup S(u^\varepsilon)$ in Y as $k \rightarrow \infty$, where $S : U \rightarrow Y$ is the fine-to-coarse scale map.*

Proof. Note that $\|y(u_k^\varepsilon)\|_Y \leq C\|q\|_H$ for $\{u_k^\varepsilon\}$, $C \in \mathbb{R}_+$ and $k \in \mathbb{N}$ as stated in Assumption 4.10. The reflexivity of Y and the Banach–Alaoglu theorem imply that $\{y(u_k^\varepsilon)\}$ admits a weakly convergent subsequence with its elements still denoted by $y(u_k^\varepsilon)$. Let $\hat{y} \in Y$ denote that weak limit. Rearranging terms in (4.18), we obtain

$$b_{\mathcal{L}}[u^\varepsilon](y(u_k^\varepsilon), v) + \int_{\Omega} (\widetilde{\mathbf{K}}[u_k^\varepsilon] - \widetilde{\mathbf{K}}[u^\varepsilon]) \nabla y(u_k^\varepsilon) \cdot \nabla v \, dx = \int_{\Omega} qv \, dx, \quad \forall v \in Y.$$

Note that $b_{\mathcal{L}}[u^\varepsilon](y(u_k^\varepsilon), v) \rightarrow b_{\mathcal{L}}[u^\varepsilon](\hat{y}, v)$ as $k \rightarrow \infty$ for all $v \in Y$, since $\mathcal{L}[u^\varepsilon] \in L(Y, Y^*)$ and hence it is weakly continuous. The continuity (4.20) and the Cauchy–Schwarz inequality yield

$$\int_{\Omega} (\widetilde{\mathbf{K}}[u_k^\varepsilon] - \widetilde{\mathbf{K}}[u^\varepsilon]) \nabla y(u_k^\varepsilon) \cdot \nabla v \, dx \leq C \|u_k^\varepsilon - u^\varepsilon\|_U \|q\|_H \|v\|_Y \rightarrow 0 \text{ as } k \rightarrow \infty,$$

since $C \in \mathbb{R}_+$ does not depend on u_k^ε and u^ε . This shows that $\hat{y} = y(u^\varepsilon)$. \square

The continuity of $S' : B_{\bar{r}^\varepsilon}(u^\varepsilon) \subset U \rightarrow L(U, Y)$ can be established through standard techniques, which we briefly outline here by examining the sensitivity equation. The sensitivity $z := S'(u)h \in Y$ of $S(\cdot)$ at $u \in B_{\bar{r}^\varepsilon}(u^\varepsilon)$ in the direction $h \in U$ is given as the solution of the linearized state equation

$$(4.27) \quad \langle e_y(y(u), u)z, v \rangle_{Y^*, Y} = -\langle e_u(y(u), u)h, v \rangle_{Y^*, Y} \quad \forall v \in Y,$$

where the partial derivatives $e_y(y, u) : Y \rightarrow Y^*$ and $e_u(y, u) : U \rightarrow Y^*$ read

$$\langle e_y(y, u)w, v \rangle_{Y^*, Y} = \int_{\Omega} \widetilde{\mathbf{K}}[u] \nabla w \cdot \nabla v \, dx, \quad \langle e_u(y, u)h, v \rangle_{Y^*, Y} = \int_{\Omega} \widetilde{\mathbf{K}}_u[h] \nabla y \cdot \nabla v \, dx,$$

respectively, and $\widetilde{\mathbf{K}}_u[h] \in \mathbb{R}^{2 \times 2}$ is given by $(\widetilde{\mathbf{K}}_u[h])_{11} = \int_{\Omega} \mathbf{K}^\varepsilon \partial_{x_1} h \, dx$ and $(\widetilde{\mathbf{K}}_u[h])_{21} = (\widetilde{\mathbf{K}}_u[h])_{12} = (\widetilde{\mathbf{K}}_u[h])_{22} = 0$ with $\|\widetilde{\mathbf{K}}_u[h]\| \leq |\Omega|^{1/2} \beta \|h\|_U$ for $h \in U$. Here, Proposition 4.9 or Assumption 4.10 implies that $e_y(y, u)$ is boundedly invertible for all $u \in B_{\bar{r}^\varepsilon}(u^\varepsilon)$, verifying Assumption 3.5 for the self-adjoint operator $\mathcal{L}[u]$. For $u_1, u_2 \in B_{\bar{r}^\varepsilon}(u^\varepsilon)$, let $z_1 = S'(u_1)h$ and $z_2 = S'(u_2)h$. Invoking the well-posedness of (4.27) and (4.20) while estimating the right-hand side of (4.27) provide us with the estimate

$$\|(S'(u_1) - S'(u_2))h\|_Y \leq C_{S'} \|u_1 - u_2\|_U \|h\|_U,$$

where $C_{S'} \in \mathbb{R}_+$ generally depends on u . Therefore, $S(u)$ is continuously Fréchet differentiable and Assumption 3.4 holds true.

4.3. Implementation issues. We provide the implementation details of Algorithm 3.1 for problem (4.11) with a periodic coefficient $\mathbf{K}^\varepsilon(x)$. Firstly, the derivative $e_\theta(y, \theta) \in L(\mathbb{R}^{N_n}, Y^*)$ is given by

$$\langle e_\theta(y, \theta) \mathbf{s}, v \rangle_{Y^*, Y} = \int_{\Omega} \widetilde{\mathbf{K}}_\theta[\mathbf{s}] \nabla y \cdot \nabla v \, dx, \quad \widetilde{\mathbf{K}}_\theta[\mathbf{s}] = \int_{\Omega} \mathbf{K}^\varepsilon \langle \nabla_\theta (\partial_{x_1} v_{\theta, n}), \mathbf{s} \rangle_{\mathbb{R}^{N_n}} \, dx$$

for $\mathbf{s} \in \mathbb{R}^{N_n}$. Given the k -th unit vector $\mathbf{e}_k \in \mathbb{R}^{N_n}$, one obtains

$$(4.28) \quad \langle y'(\theta)^* \partial_y J(y(\theta), \theta), \mathbf{e}_k \rangle_{\mathbb{R}^{N_n}} = \langle e_\theta(y(\theta), \theta) \mathbf{e}_k, p \rangle_{Y^*, Y}.$$

The formula (4.28) is useful for the assembly of the first summand in (3.13). The algebraic FE systems are described in Section 2, but we note that $\mathbb{B}_h[\theta] = \widetilde{\mathbf{K}}[v_{\theta, n}]_{\mathbb{A}_h}$ with $(\mathbb{A}_h)_{ij} := \langle \nabla \phi_i, \nabla \phi_j \rangle_H$. The discrete counterpart of (4.28) is given by

$$\langle e_\theta(y_h(\theta), \theta) \mathbf{e}_k, p_h \rangle_{Y^*, Y} = \mathbf{y}_h^T \mathbb{E}_h[\theta_k] \mathbf{p}_h, \quad 1 \leq k \leq N_n,$$

where $\mathbb{E}_h[\theta_k] \in \mathbb{R}^{N_h \times N_h}$, $(\mathbb{E}_h[\theta_k])_{ij} := \langle e_\theta(\phi_i, \theta) \mathbf{e}_k, \phi_j \rangle_{Y^*, Y}$. We get $(\mathbb{E}_h[\theta])_{ij} = \widetilde{\mathbf{k}}_M[\theta](\mathbb{A}_h)_{ij}$, where $\widetilde{\mathbf{k}}_M[\theta] \in \mathbb{R}^{N_n}$ represents approximations of $\widetilde{\mathbf{K}}_\theta[\mathbf{e}_k]$ by the Monte-Carlo approach and using the residual collocation points

$$(\widetilde{\mathbf{k}}_M[\theta])_j = \frac{1}{M_\Omega} \sum_{i=1}^{M_\Omega} \mathbf{K}^\varepsilon(x_{1,i}^r, x_{2,i}^r) \frac{\partial^2 v_{\theta, n}^M(x_{1,i}^r, x_{2,i}^r)}{\partial \theta_j \partial x_1}, \quad 1 \leq j \leq n.$$

We also use a multiscale Fourier feature network [61, 65] to reduce the effect of spectral bias. This architecture includes Fourier feature mappings $\mathcal{F}^{(k)} : \mathbb{R} \rightarrow \mathbb{R}^{2m}$:

$$\mathcal{F}^{(k)}(x) = (\cos(2\pi \mathbf{B}^{(k)} x), \sin(2\pi \mathbf{B}^{(k)} x)), \quad 1 \leq k \leq K,$$

where each entry of $\mathbf{B}^{(k)} \in \mathbb{R}^{m \times d}$ is sampled from a Gaussian distribution $\mathcal{N}(0, \varrho_k^2)$ with $\varrho_k > 0$ a specified hyperparameter. These features are used as inputs for the hidden layers, which are defined for $1 \leq k \leq K$ and $2 \leq l \leq L-1$ as follows:

$$z_1^{(k)} = \sigma(W_1 \mathcal{F}^{(k)}(x) + b_1), \quad z_l^{(k)} = \sigma(W_l z_{l-1}^{(k)} + b_l).$$

Next, the above outputs are concatenated within the linear layer as follows:

$$v_{\theta, n}^M = W_L [z_L^{(1)}, \dots, z_L^{(K)}] + b_L,$$

where W_L and b_L are the weights and biases of the output layer. To enforce the boundary conditions exactly [42, 47, 60], one may set $v_{\theta, n}^{l, M} := l(x) v_{\theta, n}^M$, where l is the corresponding signed distance function for $\partial\Omega$.

4.4. Numerical results. For our numerical experiments, we use the following setup unless otherwise specified. The multiscale Fourier feature network (Ms-PINN) is used as the main architecture of choice, with the two Fourier features initialized by $\varrho_1 = 1$ and $\varrho_2 = 1/\varepsilon$, two hidden layers with 128 neurons each, and $\tanh(x)$ as the activation functions. The full batch is used for training with the Adam algorithm [40], and $\beta_1^{Ad} = 0.9$ and $\beta_2^{Ad} = 0.999$ are chosen as the hyperparameters. The learning rate for the exponential learning rate schedule is initialized as $lr(0) = 5e - 4$, with a decay-rate of 0.75 every 1000 training iterations. For PINNs and our hybrid approach, we use automatic loss balancing [63, Algorithm 1(c)] at every 100 steps. We choose (2.10) for coupling, the uniform quadrature rule for (3.25), and $\delta = \varepsilon$ for (3.26). To reduce computational costs, we update the coarse-scale information only if $|\widetilde{\mathbf{K}}[v_{\boldsymbol{\theta}^{(it+T_K),n}}^M] - \widetilde{\mathbf{K}}[v_{\boldsymbol{\theta}^{(it),n}}^M]| > 10^{-2}$, where $T_K = 100$. Our implementation is based on JAX [8] and FEniCS Dolphin [45].

The following example is used to illustrate the concept of upscaling consistency:

$$(4.29) \quad -\partial_x(\mathbf{K}^\varepsilon \partial_x u^\varepsilon) = f^\varepsilon, \quad \text{in } \Omega := (0, 1), \quad \text{and} \quad u^\varepsilon(0) = 0, \quad u^\varepsilon(1) = 0,$$

where $\mathbf{K}^\varepsilon(x) = 2 + \sin(2\pi\varepsilon^{-1}x)$, $f^\varepsilon := q + \partial_x \mathbf{K}^\varepsilon$ and $q = -3(2x - 1)$. Then, $\widetilde{\mathbf{K}}[u] = \int_0^1 \mathbf{K}^\varepsilon(\partial_x u + 1) dx$ and $\mathbf{K}^* = (\int_0^1 \frac{dx}{\mathbf{K}^\varepsilon(x)})^{-1} = \sqrt{3} \approx 1.732$, see [37, Section 1.2] for the latter. For $\varepsilon = 1/15$ and $\varepsilon = 0.01$, we get $\widetilde{\mathbf{K}}[u_h^\varepsilon] \approx 1.733$ and $\widetilde{\mathbf{K}}[u_h^\varepsilon] \approx 1.732$, where u_h^ε are computed using finite elements on equidistant meshes with $h = 5 \cdot 10^{-4}$ and $h = 2 \cdot 10^{-4}$, respectively (these meshes are further used for validation). Then, the influence caused by an upscaling method in Assumption 2.8 is negligible in the context of Theorem 2.11. Setting $it_{\max} = 2 \cdot 10^5$, we use $M_\Omega = 2000$ and $M_\Omega = 5000$ uniformly random collocation points for $\varepsilon = 1/15$ and $\varepsilon = 0.01$ (both with hard boundary constraints), respectively, and the mesh size $h = 0.004$ for the coarse-scale problem. We use $l(x) = 4x(1 - x)$ for hard boundary constraints imposition.

If ε is not small enough, one expects an upscaling consistency gap between $y_h(u)$ and $\widetilde{Q}_\delta u$ for $u = u_h^\varepsilon$, and this gap is typically overfitted by a neural network $u = v_{\boldsymbol{\theta},n}^M$. This overfitting can introduce discrepancies in the PDE residual of (3.1). The latter can impede the route to convergence on a fine scale, rendering it generally not possible. Indeed, for $\varepsilon = 1/15$ in (4.29), we observe in Fig 1(c) that the relative L^2 error of the hybrid solver oscillates around 0.3 on our validation set, and does not drop significantly below that value, compared to the standard Ms-PINN approach without coarse-scale constraints, which shows $\sim 10^{-2}$ accuracy. We can see in Fig 1(b) that $y_h(v_{\boldsymbol{\theta},n}^M)$ matches $y_h(u_h^\varepsilon)$ well, but $\widetilde{Q}_\delta v_{\boldsymbol{\theta},n}^M$ is much closer to $y_h(v_{\boldsymbol{\theta},n}^M)$ compared to $\widetilde{Q}_\delta u_h^\varepsilon$, thus violating the upscaling consistency and causing a significant approximation error in Fig 1(a).

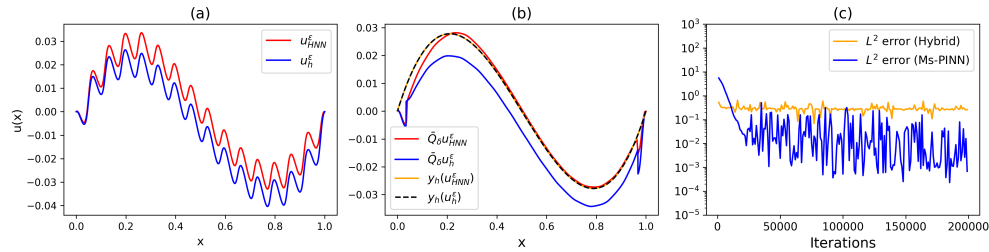


FIG. 1. Results for $\varepsilon = 1/15$, 1D problem: (a) Hybrid fine-scale solution u_{HNN}^ε and FEM solution u_h^ε , (b) Predicted state $y_h(u_{HNN}^\varepsilon)$, true discrete state $y_h(u_h^\varepsilon)$, compression $\widetilde{Q}_\delta u_{HNN}^\varepsilon$ and $\widetilde{Q}_\delta u_h^\varepsilon$, c Relative L^2 error of the hybrid solver and Ms-PINN vs iterations.

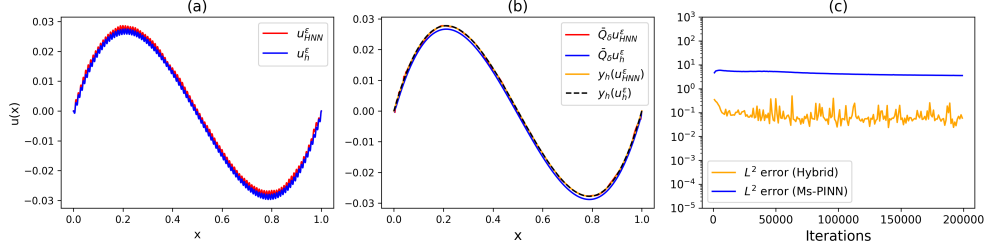


FIG. 2. Results for $\varepsilon = 0.01$, 1D problem: same description as for Fig 1.

Theorem 2.11 shows that the upscaling consistency gap decreases with decreasing ε , thus softening the conflict between the PDE residual term and the coupling term in the optimization and reducing the effect of coarse-scale overfitting. Indeed, we observe a smaller gap between $y_h(u_h^\varepsilon)$ and $\bar{Q}_\delta u_h^\varepsilon$ for $\varepsilon = 0.01$ in Fig 2(b), and a lower resulting L^2 error for the hybrid method in Fig 2(c), compared to the previous example. In addition, the hybrid solver outperforms the Ms-PINN approach by almost two orders of magnitude in terms of relative error. However, the hybrid solver error still oscillates around 0.1: there is a visible overfitting of the coarse-scale component at $x \approx 0.2$ and $x \approx 0.8$ in Fig 2(b), which causes visible approximation errors in Fig 2(a) at the same spatial points for the fine-scale hybrid approximation.

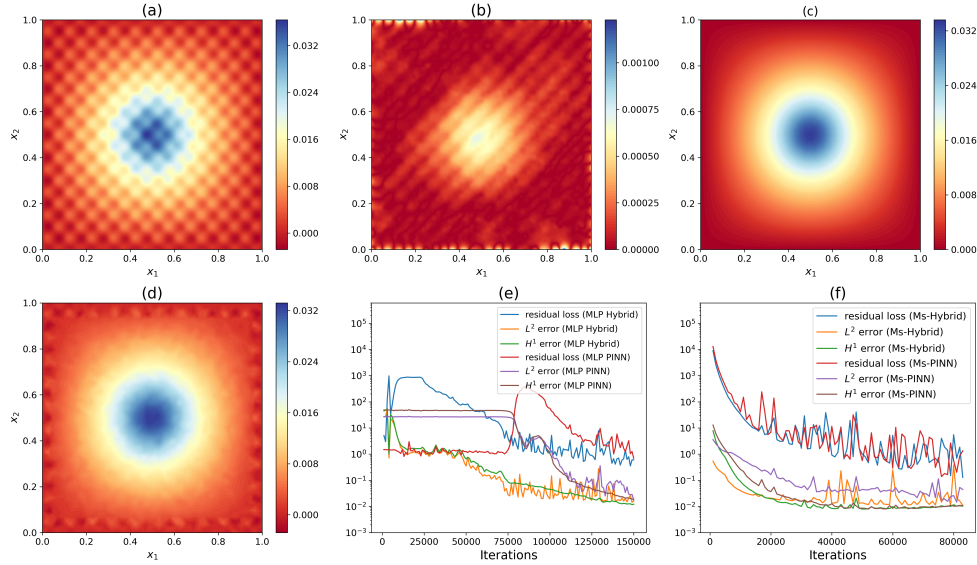


FIG. 3. Results for $\varepsilon = 0.1$, 2D problem: (a) Hybrid MLP-based fine-scale solution u_{HNN}^ε , (b) Pointwise error $|u_{HNN}^\varepsilon(x) - u_h^\varepsilon(x)|$, (c) Predicted state $y_h(u_{HNN}^\varepsilon)$, (d) Compression $\bar{Q}_\delta u_{HNN}^\varepsilon$, (e) The PDE residual losses and relative L^2 and H^1 errors vs iterations for the MLP-based hybrid solver and the MLP PINN, (f) The PDE residual losses and relative L^2 and H^1 errors vs iterations for the Ms-PINN-based hybrid solver and the Ms-PINN.

Next, we study the 2D problem (4.11) with the isotropic coefficient $\mathbf{K}^\varepsilon(x) = 3 + \sin(\pi\varepsilon^{-1}x_1) + \sin(2\pi\varepsilon^{-1}x_2)$ with $\varepsilon = 0.1$ and $q(x) = 10 \exp(-100\|x - 0.5\|_2^2)$. We note that \mathbf{K}^ε is periodic, hence we need to determine $\bar{\mathbf{K}}_{11}$ only. In addition to the Ms-PINN, we employ the multilayer perceptron (MLP) PINN with 8 hidden layers with 64 neurons each for both the standard and hybrid approaches while setting $lr(0) = 1e-3$

TABLE 1

Comparison of the Ms-PINNs and the MLP-based PINNs with the hybrid method for the 2-D problem. The presented quantities are averages over 5 random initializations of NN parameters and collocation points. For the MLP PINN only one realization is presented, as all others failed to deliver reasonable results. All runs are executed on A100 GPUs with 40 GB RAM.

[H]				
Method	Rel. L^2 error	Rel. H^1 error	iterations	time (sec)
Hybrid Ms-PINN	1.28E-02 \pm 0.003	2.23E-02 \pm 0.008	77478	554
Hybrid MLP	1.42E-02 \pm 0.001	1.44E-02 \pm 0.008	139400	1725
Ms-PINN	1.97E-02 \pm 0.005	2.20E-02 \pm 0.005	70009	354
MLP PINN	1.71E-02 \pm 1.000	1.89E-02 \pm 1.000	150000	1221

for the initial learning rate. We use $M_\Omega = 25000$ and $M_{\partial\Omega}=2500$ uniformly random collocation points and the mesh size $h \approx 0.04$ for the coarse-scale discretization. Figure 3 shows exemplary realizations of the hybrid solver. The MLP network, prone to low-frequency bias, benefits from embedding coarse-scale constraints, which accelerates the approximation of the coarse-scale component and mitigates the bias, as seen in Fig 3(e). The MLP approach struggles with being trapped at poor local minima, failing to provide a reasonable approximation for around 75k iterations. In contrast, the hybrid approach exhibits steadily decreasing residuals and errors. For the Ms-PINNs, the hybrid method also shows faster decay of the L^2 and H^1 relative errors², though the differences are less pronounced compared to the MLP approach, as the Ms-PINN approach is less prone to the spectral bias.

In Table 1, we report the L^2 and H^1 relative errors corresponding to the smallest residual norm value within the learning history, the number of iterations required to achieve it, and the compute time, all averaged over 5 random initializations. According to our selection criteria, the hybrid Ms-PINN requires slightly more iterations than the standard Ms-PINN, but in Fig 3(f) the convergence to the reported values in Table 1 is factually noticeably faster for the hybrid approach, suggesting more robustness at the cost of compute time. For the standard MLP PINN, one successful realization was obtained for Fig 3(e), while many others failed to approximate the solution. The hybrid MLP network consistently yields robust results across all realizations.

5. Conclusion. This paper focuses on the structural properties of a learning-informed PDE-constrained optimization problem with a PINN-based objective, resulting in a hybrid two-scale solver. Our approach integrates conventional multiscale methodologies and deep learning techniques, and the proposed PDE-constrained optimization setting seems particularly well-suited for this purpose. However, selecting a suitable neural network approximation scheme and developing an efficient optimization algorithm, aimed at enhancing accuracy while minimizing computational time, are both essential for further algorithmic developments. This task requires considering recent advancements in PINNs and the field of PDE-constrained optimization. For example, one may consider using non-smooth activation functions, introducing non-smoothness into the related PDE-constrained optimization. Such a setting challenges both the derivation of suitable stationarity conditions for the PDE-constrained multiscale approach and its numerical solution. A comprehensive investigation of such a setting, as well as the development of efficient optimization algorithms to address other problems, remain part of our future work in this area.

²The H^1 norm is induced by the L^2 norm of the gradient.

REFERENCES

- [1] A. ABDULLE, E. WEINAN, B. ENGQUIST, AND E. VANDEN-ELJNDEN, *The heterogeneous multi-scale method*, Acta Numerica, 21 (2012), pp. 1–87.
- [2] R. A. ADAMS AND J. J. FOURNIER, *Sobolev spaces*, Elsevier, 2003.
- [3] E. ALEXANDRE AND J.-L. GUERMOND, *Theory and practice of finite elements*, Springer, 2004.
- [4] H. ARBABI, J. E. BUNDER, G. SAMAEY, A. J. ROBERTS, AND I. G. KEVREKIDIS, *Linking machine learning with multiscale numerics: Data-driven discovery of homogenized equations*, Jom, 72 (2020), pp. 4444–4457.
- [5] S. BERRONE, C. CANUTO, AND M. PINTORE, *Variational physics informed neural networks: the role of quadratures and test functions*, Journal of Scientific Computing, 92 (2022), p. 100.
- [6] P. BOCHEV AND M. GUNZBURGER, *Least-squares methods for hyperbolic problems*, in Handbook of Numerical Analysis, vol. 17, Elsevier, 2016, pp. 289–317.
- [7] P. B. BOCHEV AND M. D. GUNZBURGER, *Least-squares finite element methods*, vol. 166, Springer Science & Business Media, 2009.
- [8] J. BRADBURY, R. FROSTIG, P. HAWKINS, M. J. JOHNSON, C. LEARY, D. MACLAURIN, G. NECULA, A. PASZKE, J. VANDERPLAS, S. WANDERMAN-MILNE, ET AL., *Jax: Composable transformations of python+ numpy programs (v0. 2.5)*, Software available from <https://github.com/google/jax>, (2018).
- [9] S. C. BRENNER, *The mathematical theory of finite element methods*, Springer, 2008.
- [10] I. BREVIS, I. MUGA, AND K. G. VAN DER ZEE, *Neural control of discrete weak formulations: Galerkin, least squares & minimal-residual methods with quasi-optimal weights*, Computer Methods in Applied Mechanics and Engineering, 402 (2022), p. 115716.
- [11] E. CASAS, *Optimal control in coefficients of elliptic equations with state constraints*, Applied Mathematics and Optimization, 26 (1992), pp. 21–37.
- [12] F. CHALON, M. MAINGUY, P. LONGUEMARE, AND P. LEMONNIER, *Upscaling of elastic properties for large scale geomechanical simulations*, International journal for numerical and analytical methods in geomechanics, 28 (2004), pp. 1105–1119.
- [13] Y. CHEN, L. LU, G. E. KARNIADAKIS, AND L. DAL NEGRO, *Physics-informed neural networks for inverse problems in nano-optics and metamaterials*, Optics express, 28 (2020), pp. 11618–11633.
- [14] R. M. CHRISTENSEN, *Mechanics of composite materials*, Courier Corporation, 2012.
- [15] S. CUOMO, V. S. DI COLA, F. GIAMPAOLO, G. ROZZA, M. RAISSI, AND F. PICCIALI, *Scientific machine learning through physics-informed neural networks: where we are and what's next*, Journal of Scientific Computing, 92 (2022), p. 88.
- [16] T. DE RYCK, A. D. JAGTAP, AND S. MISHRA, *Error estimates for physics informed neural networks approximating the Navier-Stokes equations*, IMA Journal of Numerical Analysis, (2023).
- [17] T. DE RYCK, S. LANTHALER, AND S. MISHRA, *On the approximation of functions by tanh neural networks*, Neural Networks, 143 (2021), pp. 732–750.
- [18] Y. DIAO, J. YANG, Y. ZHANG, D. ZHANG, AND Y. DU, *Solving multi-material problems in solid mechanics using physics-informed neural networks based on domain decomposition technology*, Computer Methods in Applied Mechanics and Engineering, 413 (2023), p. 116120.
- [19] G. DONG, M. HINTERMÜLLER, AND K. PAPAITSOROS, *Optimization with learning-informed differential equation constraints and its applications*, ESAIM: Control, Optimisation and Calculus of Variations, 28 (2022), p. 3.
- [20] L. J. DURLOFSKY, *Numerical calculation of equivalent grid block permeability tensors for heterogeneous porous media*, Water resources research, 27 (1991), pp. 699–708.
- [21] Y. EFENDIEV, J. GALVIS, AND T. Y. HOU, *Generalized multiscale finite element methods (GMs-FEM)*, Journal of computational physics, 251 (2013), pp. 116–135.
- [22] R. EWING, O. ILIEV, R. LAZAROV, I. RYBAK, AND J. WILLEMS, *A simplified method for upscaling composite materials with high contrast of the conductivity*, SIAM journal on scientific computing, 31 (2009), pp. 2568–2586.
- [23] C. FARMER, *Upscaling: a review*, International journal for numerical methods in fluids, 40 (2002), pp. 63–78.
- [24] X. GLOROT AND Y. BENGIO, *Understanding the difficulty of training deep feedforward neural networks*, in Proceedings of the thirteenth international conference on artificial intelligence and statistics, JMLR Workshop and Conference Proceedings, 2010, pp. 249–256.
- [25] I. GOODFELLOW, Y. BENGIO, AND A. COURVILLE, *Deep learning*, MIT press, 2016.
- [26] S. GOSWAMI, C. ANITESCU, S. CHAKRABORTY, AND T. RABCZUK, *Transfer learning enhanced physics informed neural network for phase-field modeling of fracture*, Theoretical and Applied Fracture Mechanics, 106 (2020), p. 102447.

- [27] M. GRIEBEL AND M. KLITZ, *Homogenization and numerical simulation of flow in geometries with textile microstructures*, Multiscale Modeling & Simulation, 8 (2010), pp. 1439–1460.
- [28] P. GRISVARD, *Elliptic problems in nonsmooth domains*, SIAM, 2011.
- [29] I. GÜHRING, G. KUTYNIOK, AND P. PETERSEN, *Error bounds for approximations with deep ReLU neural networks in W^s, p norms*, Analysis and Applications, 18 (2020), pp. 803–859.
- [30] J. HAN AND Y. LEE, *A neural network approach for homogenization of multiscale problems*, Multiscale Modeling & Simulation, 21 (2023), pp. 716–734.
- [31] M. HINZE, R. PINNAU, M. ULBRICH, AND S. ULBRICH, *Optimization with PDE constraints*, vol. 23, Springer Science & Business Media, 2008.
- [32] Z. HU, K. SHUKLA, G. E. KARNIADAKIS, AND K. KAWAGUCHI, *Tackling the curse of dimensionality with physics-informed neural networks*, arXiv preprint arXiv:2307.12306, (2023).
- [33] O. ILIEV, Z. LAKDAWALA, AND V. STARIKOVICIUS, *On a numerical subgrid upscaling algorithm for Stokes–Brinkman equations*, Computers & Mathematics with Applications, 65 (2013), pp. 435–448.
- [34] O. ILIEV, R. LAZAROV, AND J. WILLEMS, *Variational multiscale finite element method for flows in highly porous media*, Multiscale modeling & simulation, 9 (2011), pp. 1350–1372.
- [35] A. D. JAGTAP AND G. E. KARNIADAKIS, *Extended physics-informed neural networks (XPINNs): A generalized space-time domain decomposition based deep learning framework for nonlinear partial differential equations.*, in AAAI Spring Symposium: MLPS, 2021, pp. 2002–2041.
- [36] A. D. JAGTAP, Z. MAO, N. ADAMS, AND G. E. KARNIADAKIS, *Physics-informed neural networks for inverse problems in supersonic flows*, Journal of Computational Physics, 466 (2022), p. 111402.
- [37] V. V. JIKOV, S. M. KOZLOV, AND O. A. OLEINIK, *Homogenization of differential operators and integral functionals*, Springer Science & Business Media, 2012.
- [38] E. KHARAZMI, Z. ZHANG, AND G. E. KARNIADAKIS, *Variational physics-informed neural networks for solving partial differential equations*, arXiv preprint arXiv:1912.00873, (2019).
- [39] E. KHARAZMI, Z. ZHANG, AND G. E. KARNIADAKIS, *hp-vpinns: Variational physics-informed neural networks with domain decomposition*, Computer Methods in Applied Mechanics and Engineering, 374 (2021), p. 113547.
- [40] D. P. KINGMA AND J. BA, *Adam: A method for stochastic optimization*, arXiv preprint arXiv:1412.6980, (2014).
- [41] F. KRÖPFL, R. MAIER, AND D. PETERSEIM, *Neural network approximation of coarse-scale surrogates in numerical homogenization*, Multiscale Modeling & Simulation, 21 (2023), pp. 1457–1485.
- [42] P. L. LAGARI, L. H. TSOUKALAS, S. SAFARKHANI, AND I. E. LAGARIS, *Systematic construction of neural forms for solving partial differential equations inside rectangular domains, subject to initial, boundary and interface conditions*, International Journal on Artificial Intelligence Tools, 29 (2020), p. 2050009.
- [43] I. E. LAGARIS, A. LIKAS, AND D. I. FOTIADIS, *Artificial neural networks for solving ordinary and partial differential equations*, IEEE transactions on neural networks, 9 (1998), pp. 987–1000.
- [44] W. T. LEUNG, G. LIN, AND Z. ZHANG, *NH-PINN: Neural homogenization-based physics-informed neural network for multiscale problems*, Journal of Computational Physics, 470 (2022), p. 111539.
- [45] A. LOGG AND G. N. WELLS, *Dolfin: Automated finite element computing*, ACM Transactions on Mathematical Software (TOMS), 37 (2010), pp. 1–28.
- [46] Z. K. LOW, N. BLAL, N. NAOUAR, AND D. BAILLIS, *Influence of boundary conditions on computation of the effective thermal conductivity of foams*, International Journal of Heat and Mass Transfer, 155 (2020), p. 119781.
- [47] L. LU, R. PESTOURIE, W. YAO, Z. WANG, F. VERDUGO, AND S. G. JOHNSON, *Physics-informed neural networks with hard constraints for inverse design*, SIAM Journal on Scientific Computing, 43 (2021), pp. B1105–B1132.
- [48] A. MÅLQVIST AND D. PETERSEIM, *Localization of elliptic multiscale problems*, Mathematics of Computation, 83 (2014), pp. 2583–2603.
- [49] H. N. MHASKAR AND N. HAHM, *Neural networks for functional approximation and system identification*, Neural Computation, 9 (1997), pp. 143–159.
- [50] S. MISHRA AND R. MOLINARO, *Estimates on the generalization error of physics-informed neural networks for approximating a class of inverse problems for PDEs*, IMA Journal of Numerical Analysis, 42 (2022), pp. 981–1022.
- [51] S. MISHRA AND R. MOLINARO, *Estimates on the generalization error of physics-informed neural*

- networks for approximating PDEs*, IMA Journal of Numerical Analysis, 43 (2022), pp. 1–43.
- [52] B. MOSELEY, A. MARKHAM, AND T. NISSEN-MEYER, *Finite basis physics-informed neural networks (fbpinns): a scalable domain decomposition approach for solving differential equations*, Advances in Computational Mathematics, 49 (2023), p. 62.
- [53] S. MOWLAVI AND S. NABI, *Optimal control of PDEs using physics-informed neural networks*, Journal of Computational Physics, 473 (2023), p. 111731.
- [54] J. S. R. PARK AND X. ZHU, *Physics-informed neural networks for learning the homogenized coefficients of multiscale elliptic equations*, Journal of Computational Physics, 467 (2022), p. 111420.
- [55] N. RAHAMAN, A. BARATIN, D. ARPIT, F. DRAXLER, M. LIN, F. HAMPRECHT, Y. BENGIO, AND A. COURVILLE, *On the spectral bias of neural networks*, in International Conference on Machine Learning, PMLR, 2019, pp. 5301–5310.
- [56] M. RAISSI, P. PERDIKARIS, AND G. E. KARNIADAKIS, *Physics-informed neural networks: A deep learning framework for solving forward and inverse problems involving nonlinear partial differential equations*, Journal of Computational physics, 378 (2019), pp. 686–707.
- [57] Y. SHIN, Z. ZHANG, AND G. E. KARNIADAKIS, *Error estimates of residual minimization using neural networks for linear PDEs*, Journal of Machine Learning for Modeling and Computing, 4 (2023).
- [58] K. SHUKLA, A. D. JAGTAP, AND G. E. KARNIADAKIS, *Parallel physics-informed neural networks via domain decomposition*, Journal of Computational Physics, 447 (2021), p. 110683.
- [59] J. SIRIGNANO, J. MACART, AND K. SPILIOPOULOS, *PDE-constrained models with neural network terms: optimization and global convergence*, Journal of Computational Physics, 481 (2023), p. 112016.
- [60] N. SUKUMAR AND A. SRIVASTAVA, *Exact imposition of boundary conditions with distance functions in physics-informed deep neural networks*, Computer Methods in Applied Mechanics and Engineering, 389 (2022), p. 114333.
- [61] M. TANCIK, P. SRINIVASAN, B. MILDENHALL, S. FRIDOVICH-KEIL, N. RAGHAVAN, U. SINGHAL, R. RAMAMOORTHY, J. BARRON, AND R. NG, *Fourier features let networks learn high frequency functions in low dimensional domains*, Advances in Neural Information Processing Systems, 33 (2020), pp. 7537–7547.
- [62] J. M. TAYLOR, D. PARDO, AND I. MUGA, *A deep fourier residual method for solving PDEs using neural networks*, Computer Methods in Applied Mechanics and Engineering, 405 (2023), p. 115850.
- [63] S. WANG, S. SANKARAN, H. WANG, AND P. PERDIKARIS, *An expert's guide to training physics-informed neural networks*, arXiv preprint arXiv:2308.08468, (2023).
- [64] S. WANG, Y. TENG, AND P. PERDIKARIS, *Understanding and mitigating gradient flow pathologies in physics-informed neural networks*, SIAM Journal on Scientific Computing, 43 (2021), pp. A3055–A3081.
- [65] S. WANG, H. WANG, AND P. PERDIKARIS, *On the eigenvector bias of fourier feature networks: From regression to solving multi-scale PDEs with physics-informed neural networks*, Computer Methods in Applied Mechanics and Engineering, 384 (2021), p. 113938.
- [66] S. WANG, X. YU, AND P. PERDIKARIS, *When and why PINNs fail to train: A neural tangent kernel perspective*, Journal of Computational Physics, 449 (2022), p. 110768.
- [67] E. WEINAN, B. ENQUIST, AND Z. HUANG, *Heterogeneous multiscale method: a general methodology for multiscale modeling*, Physical Review B, 67 (2003), p. 092101.
- [68] X.-H. WU, Y. EFENDIEV, AND T. Y. HOU, *Analysis of upscaling absolute permeability*, Discrete & Continuous Dynamical Systems-B, 2 (2002), p. 185.
- [69] T. XIE AND F. CAO, *The errors of simultaneous approximation of multivariate functions by neural networks*, Computers & Mathematics with Applications, 61 (2011), pp. 3146–3152.
- [70] C. XU, B. T. CAO, Y. YUAN, AND G. MESCHKE, *Transfer learning based physics-informed neural networks for solving inverse problems in engineering structures under different loading scenarios*, Computer Methods in Applied Mechanics and Engineering, 405 (2023), p. 115852.
- [71] D. YAROTSKY, *Error bounds for approximations with deep ReLU networks*, Neural Networks, 94 (2017), pp. 103–114.
- [72] Y. ZANG, G. BAO, X. YE, AND H. ZHOU, *Weak adversarial networks for high-dimensional partial differential equations*, Journal of Computational Physics, 411 (2020), p. 109409.
- [73] M. ZEINHOFER, R. MASRI, AND K.-A. MARDAL, *A unified framework for the error analysis of physics-informed neural networks*, arXiv preprint arXiv:2311.00529, (2023).
- [74] E. ZHANG, M. DAO, G. E. KARNIADAKIS, AND S. SURESH, *Analyses of internal structures and defects in materials using physics-informed neural networks*, Science advances, 8 (2022),

p. eabk0644.